Agilent
Fundamentals of RF and Microwave Power Measurements (Part 2)

Power Sensors and Instrumentation

Application Note 1449-2

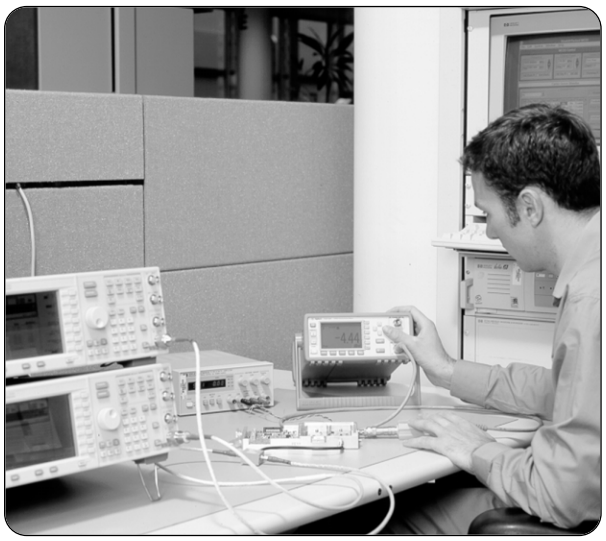

Agilent Technologies

For user convenience, Agilent's *Fundamentals of RF and Microwave Power Measurements*, application note 64-1, literature number 5965-6330E, has been updated and segmented into four technical subject groupings. The following abstracts explain how the total field of power measurement fundamentals is now presented.

Fundamentals of RF and Microwave Power Measurements (Part 1)

Introduction to Power, History, Definitions, International Standards, and Traceability

AN 1449-1, literature number 5988-9213EN

Part 1 introduces the historical basis for power measurements, and provides definitions for average, peak, and complex modulations. This application note overviews various sensor technologies needed for the diversity of test signals. It describes the hierarchy of international power traceability, yielding comparison to national standards at worldwide National Measurement Institutes (NMIs) like the U.S. National Institute of Standards and Technology. Finally, the theory and practice of power sensor comparison procedures are examined with regard to transferring calibration factors and uncertainties. A glossary is included which serves all four parts.

Fundamentals of RF and Microwave Power Measurements (Part 2)

Power Sensors and Instrumentation

AN 1449-2, literature number 5988-9214EN

Part 2 presents all the viable sensor technologies required to exploit the users' wide range of unknown modulations and signals under test. It explains the sensor technologies, and how they came to be to meet certain measurement needs. Sensor choices range from the venerable thermistor to the innovative thermocouple to more recent improvements in diode sensors. In particular, clever variations of diode combinations are presented, which achieve ultra-wide dynamic range and square-law detection for complex modulations. New instrumentation technologies, which are underpinned with powerful computational processors, achieve new data performance.

Fundamentals of RF and Microwave Power Measurements (Part 3)

Power Measurement Uncertainty per International Guides

AN 1449-3, literature number 5988-9215EN

Part 3 discusses the all-important theory and practice of expressing measurement uncertainty, mismatch considerations, signal flowgraphs, ISO 17025, and examples of typical calculations. Considerable detail is shown on the ISO 17025, *Guide for the Expression of Measurement Uncertainties*, has become the international standard for determining operating specifications. Agilent has transitioned from ANSI/NCSL Z540-1-1994 to ISO 17025.

Fundamentals of RF and Microwave Power Measurements (Part 4)

An Overview of Agilent Instrumentation for RF/Microwave Power Measurements

AN 1449-4, literature number 5988-9216EN

Part 4 overviews various instrumentation for measuring RF and microwave power, including spectrum analyzers, microwave receivers, network/spectrum analyzers, and the most accurate method, power sensors/meters. It begins with the unknown signal, of arbitrary modulation format, and draws application-oriented comparisons for selection of the best instrumentation technology and products.

Most of the chapter is devoted to the most accurate method, power meters and sensors. It includes comprehensive selection guides, frequency coverages, contrasting accuracy and dynamic performance to pulsed and complex digital modulations. These are especially crucial now with the advances in wireless communications formats and their statistical measurement needs.

Table of Contents

Introduction

The purposes of the new series of *Fundamentals of RF and Microwave Power Measurements* application notes, which were leveraged from former note AN 64-1, is to

1) Retain tutorial information about historical and fundamental considerations of RF/microwave power measurements and technology which tend to remain timeless.

2) Provide current information on new meter and sensor technology.

3) Present the latest modern power measurement techniques and test equipment that represents the current state-of-the-art.

Part 2 of this series, *Power Sensors and Instrumentation*, is a comprehensive overview of the broad array of power sensors and instrumentation available today.

Chapter 2 starts with a brief look at the classic thermistor sensor and dc-substitution meter technology. Since thermistors remain the predominant method to trace standard power from National Measurement Institutes such as the National Institute of Standards and Technology (NIST), Agilent maintains a significant line of such products.

Chapter 3 introduces the thermocouple sensors and instruments that came on the scene in the early 1970s. They featured a truly dramatic increase in range and lowered uncertainty of measurements because the sensors featured full square-law conversion and wider dynamic range. They had significantly lower SWR, which reduced measurement uncertainty greatly. And they were far more rugged than thermistors. Soon, Agilent enhanced them by combining with integral, calibrated attenuators for accepting input powers up to 25 watts.

Chapter 4 describes the theory and practice of diode-based power sensors. Although diodes were used for power detection as far back as World War II, it took Agilent's introduction of the 8484A diode power sensor in 1975 to provide broadband matching to the coaxial structure and temperature isolation from external elements to make the technology succeed. Since diodes were 30 dB more sensitive, and also exhibited true square conversion for about the lowest 50 dB of range, they quickly achieved an important place in user requirements.

Chapter 5 presents the latest technology for applying diode sensors to characterization of RF/microwave signals with complex modulation typical of wireless systems, or pulsed formats typical of radar and navigation systems. Such complex modulations required wider-bandwidth instrumentation to accommodate the fast pulses and wideband digital modulations of the wireless technologies. But, in addition, new microprocessor-based technology plus the digital sampling data capture of the new instrumentation permitted dramatic expansion of computed characterization of power, such as peak-to-average ratios. New research data is provided for peak and average sensor linearity and pulse shape characterization.

Note: In this application note, numerous technical references will be made to the other published parts of the *Fundamentals of RF And Microwave Power Measurements* series. For brevity, we will use the format *Fundamentals Part X*. This should insure that you can quickly locate the concept in the other publication. Brief abstracts for the four-part series are provided on the inside front cover.

II. Thermistor Sensors and Instrumentation

Bolometer sensors, especially thermistors, have held an important historical position in RF/microwave power measurements. However, in recent years thermocouple and diode technologies have captured the bulk of those applications because of their increased sensitivities, wider dynamic ranges, and higher power capabilities. Yet, thermistors are still the sensor of choice for power transfer standards because of their DC power substitution capability. The following material reviews the basic theory and operation of thermistor sensors and their associated dual-balanced bridge power meter instruments.

Bolometers are power sensors that operate by changing resistance due to a change in temperature. The change in temperature results from converting RF or microwave energy into heat within the bolometric element. There are two principle types of bolometers, barretters and thermistors. A barretter is a thin wire that has a positive temperature coefficient of resistance. Thermistors are semiconductors with a negative temperature coefficient. Barretters are no longer used.

The thermistor sensor used for RF power measurement is a small bead of metallic oxides, typically 0.4 mm diameter with 0.03 mm diameter wire leads. Thus the balanced-bridge technique always maintains the thermistor element at a constant resistance, R, by means of DC or low frequency AC bias. As RF power is dissipated in the thermistor, tending to lower R, the bias power is withdrawn by an equal amount to balance the bridge and keep R the same value. That decrease in bias power is then displayed on a meter to indicate RF power.

Thermistor sensors

Thermistor elements are mounted in coaxial structures so they are compatible with common transmission line systems used at microwave and RF frequencies. Modern thermistor sensors have a second set of compensating thermistors to correct for ambient temperature variations.

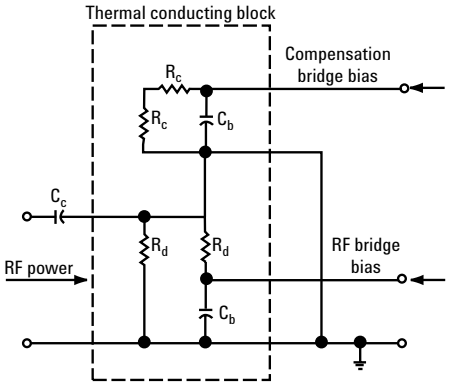

Figure 2-1. 478A coaxial sensor simplified diagram

Coaxial thermistor sensors

The Agilent 478A and 8478B thermistor mounts (thermistor mount was the earlier name for sensor) contain four matched thermistors and measure power from 10 MHz to 10 and 18 GHz. The two RF-detecting thermistors, bridge-balanced to 100 Ω each, are connected in series (200 Ω) as far as the DC bridge circuits are concerned. For the RF circuit, the two thermistors appear to be connected in parallel, presenting a 50 Ω impedance to the test signal. The principle advantage of this connection scheme is that both RF thermistor leads to the bridge are at RF ground. See Figure 2-1.

Compensating thermistors, which monitor changes in ambient temperature but not changes in RF power, are also connected in series. These thermistors are also biased to a total of 200 Ω by a second bridge in the power meter, called the compensating bridge. The compensating thermistors are completely enclosed in a cavity for electrical isolation from the RF signal but they are mounted on the same thermal conducting block as the detecting thermistors. The thermal mass of the block is large enough to prevent sudden temperature gradients between the thermistors. This improves the isolation of the system from thermal inputs such as human hand effects.

There is a particular error, called dual element error, that is limited to coaxial thermistor mounts where the two thermistors are in parallel for the RF energy, but in series for DC. If the two thermistors are not quite identical in resistance, then more RF current will flow in the one of least resistance, but more DC power will be dissipated in the one of greater resistance. The lack of equivalence in the dissipated DC and RF power is a minor source of error that is proportional to power level. For thermistor sensors, this error is less than 0.1% at the high power end of their measurement range and is therefore considered as insignificant in the uncertainty analysis of *Fundamentals Part 3*.

Bridges, from Wheatstone to dual-compensated DC types

Over the decades, power bridges for monitoring and regulating power sensing thermistors have gone through a major evolution. Early bridges such as the simple Wheatstone type were manually balanced. Automatically-balanced bridges, such as the 430C of 1952, provided great improvements in convenience but still had limited dynamic range due to thermal drift on their 30 µW (full scale) range. In 1966, with the introduction of the first temperature-compensated meter, the 431A, drift was reduced so much that meaningful measurements could be made down to 1 µW.[1]

The Agilent 432A power meter uses DC to maintain balance in both bridges. The 432A has the further convenience of an automatic zero set, eliminating the need for the operator to precisely reset zero for each measurement.

The 432A features an instrumentation accuracy of 1%. It also provides the ability to externally measure the internal bridge voltages with external higher accuracy DC voltmeters, thus permitting a higher accuracy level for power transfer techniques to be used. In the 432A, thermo-electric voltages are so small, compared to the metered voltages, as to be insignificant.

The principal parts of the 432A (Figure 2-2) are two self-balancing bridges, the meter-logic section, and the auto-zero circuit. The RF bridge, which contains the detecting thermistor, is kept in balance by automatically varying the DC voltage V_{rf}, which drives that bridge. The compensating bridge, which contains the compensating thermistor, is kept in balance by automatically varying the DC voltage V_c, which drives that bridge.

The power meter is initially zero-set (by pushing the zero-set button) with no applied RF power by making V_c equal to V_{rfo} (V_{rfo} means V_{rf} with zero RF power). After zero-setting, if ambient temperature variations change thermistor resistance, both bridge circuits respond by applying the same new voltage to maintain balance.

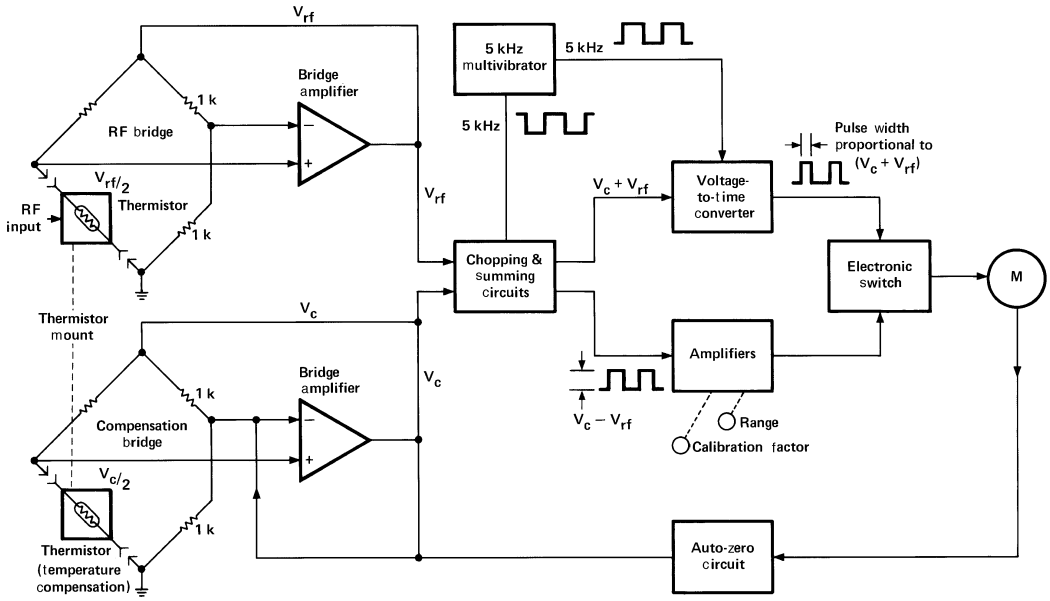

Figure 2-2. Simplified diagram of the 432A power meter.

If RF power is applied to the detecting thermistor, V_{rf} decreases so that

$$P_{rf} = \frac{V_{rfo}^2}{4R} - \frac{V_{rf}^2}{4R} \qquad \text{(Equation 2-1)}$$

where P_{rf} is the RF power applied and R is the value of the thermistor resistance at balance, but from zero-setting, $V_{rfo} = V_c$ so that

$$P_{rf} = \frac{1}{4R} (V_c^2 - V_{rf}^2) \qquad \text{(Equation 2-2)}$$

which can be written

$$P_{rf} = \frac{1}{4R} (V_c - V_{rf}) (V_c + V_{rf}) \qquad \text{(Equation 2-3)}$$

The meter logic circuitry is designed to meter the voltage product shown in Equation 2-3. Ambient temperature changes cause V_c and V_{rf} to change so there is zero change to $V_c^2 - V_{rf}^2$ and therefore no change to the indicated P_{rf}.

As seen in Figure 2-2, some clever analog circuitry is used to accomplish the multiplication of voltages proportional to $(V_c - V_{rf})$ and $(V_c + V_{rf})$ by use of a voltage-to-time converter. In these days, such simple arithmetic would be performed by the ubiquitous microprocessor, but the 432A predated that technology and performs well without it.

The principal sources of instrumentation uncertainty of the 432A lie in the metering logic circuits. But V_{rf} and V_c are both available at the rear panel of the 432A. With precision digital voltmeters and proper procedure, those outputs allow the instrumentation uncertainty to be reduced to ±0.2% for many measurements. The procedure is described in the operating manual for the 432A.

Thermistors as power transfer standards

Almost 100% of the popularity of the Agilent 432A is driven by its unique use as an adjunct to transferring power standards from NMIs to secondary standards labs and production facilities. The DC substitution technique has been accepted by standards labs the world over, for tracing power uncertainties and calibration factors from complex microcalorimeters in pristine primary labs to field measurements. This alleviates the necessity for every organization in the world to build, maintain and feed those complex microcalorimeters.

The use of thermistor sensors permits highly accurate and repeatable measurements of calibration factor, since the DC can be measured to very low uncertainty with external instruments such as digital voltmeters. The sensors are highly portable, the cal factors are stable over time, and the technologies are accepted by common usage all over the world.

Regular use is also made of “round robins” between various user groups of companies, whereby an artifact sensor is moved from one secondary standards lab to another, all coordinated by a “pivot lab.” When finished, all measured data are combined and analyzed from start to finish, yielding specific performance data on the individual participating labs, both for equipment and for their measuring procedures.

Detailed descriptions of the use of thermistor sensors in the power transfer process are found in *Fundamentals Part 1*, under Chapter III on the hierarchy and traceability of power. It is not included here because the theory and practice of sensor calibration and tracing of power standards are part of the same system considerations.

---

[1] Pramann, R.F. “A Microwave Power Meter with a Hundredfold Reduction in Thermal Drift,” Hewlett-Packard Journal, Vol. 12, No. 10 (June, 1961).

III. Thermocouple Sensors and Instrumentation

Thermocouple sensors have been the detection technology of choice for sensing RF and microwave power since their introduction in 1974. The two main reasons for this evolution are: 1) they exhibit higher sensitivity than previous thermistor technology, and 2) they feature an inherent square-law detection characteristic (input RF power is proportional to DC voltage out).

Since thermocouples are heat-based sensors, they are true "averaging detectors." This recommends them for all types of signal formats from continuous wave (CW) to complex digital phase modulations. In addition, they are more rugged than thermistors, make useable power measurements down to 0.3 µW (–30 dBm, full scale), and have lower measurement uncertainty because of better voltage standing wave radio (SWR).

The evolution to thermocouple technology is the result of combining thin-film and semiconductor technologies to give a thoroughly understood, accurate, rugged, and reproducible power sensor. This chapter briefly describes the principles of thermocouples, the construction and design of modern thermocouple sensors, and the instrumentation used to measure their rather tiny sensor DC-output levels.

Principles of thermocouples

Thermocouples are based on the fact that dissimilar metals generate a voltage due to temperature differences at a hot and a cold junction of the two metals. As a simple example of the physics involved, imagine a long metal rod that is heated at the left end as in Figure 3-1. Because of the increased thermal agitation at the left end, many additional electrons become free from their parent atoms. The increased density of free electrons at the left causes diffusion toward the right. There is also a force attempting to diffuse the positive ions to the right but the ions are locked into the metallic structure and cannot migrate. So far, this explanation has not depended on Coulomb forces. The migration of electrons toward the right is by diffusion, the same physical phenomenon that tends to equalize the partial pressure of a gas throughout a space.

Each electron that migrates to the right leaves behind a positive ion. That ion tends to attract the electron back to the left with a force given by Coulomb's law. The rod reaches equilibrium when the rightward force of heat-induced diffusion is exactly balanced by the leftward force of Coulomb's law. The leftward force can be represented by an electric field pointing toward the right. The electric field, summed up along the length of the rod, gives rise to a voltage source called the Thomson electromotive force (emf). This explanation is greatly simplified but indicates the principle.

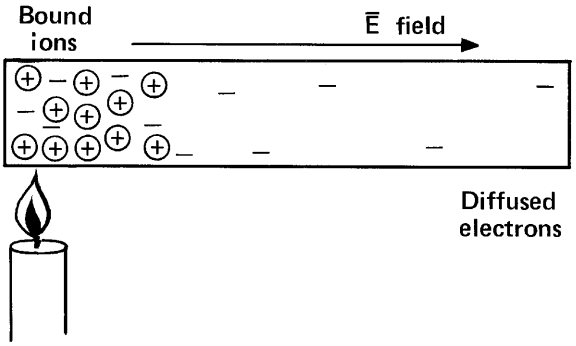

Figure 3-1. Heat at one end of a metal rod gives rise to an electric field.

The same principles apply at a junction of dissimilar metals where different free electron densities in the two different metals give rise to diffusion and an emf. The name of this phenomenon is the Peltier effect.

A thermocouple is usually a loop or circuit of two different materials as shown in Figure 3-2. One junction of the metals is exposed to heat, the other is not. If the loop remains closed, current will flow in the loop as long as the two junctions remain at different temperatures. If the loop is broken to insert a sensitive volt-meter, it will measure the net emf. The thermocouple loop uses both the Thomson emf and the Peltier emf to produce the net thermoelectric voltage. The total effect is also known as the Seebeck emf.

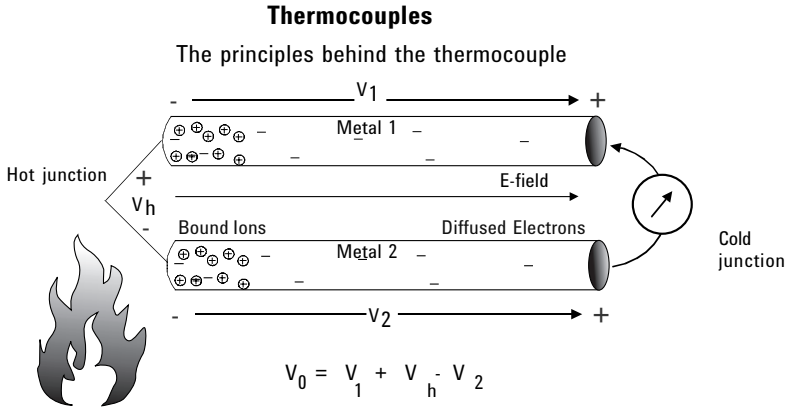

Figure 3-2. Total thermocouple output is the resultant of several thermoelectrical voltages generated along the two-metal circuit.

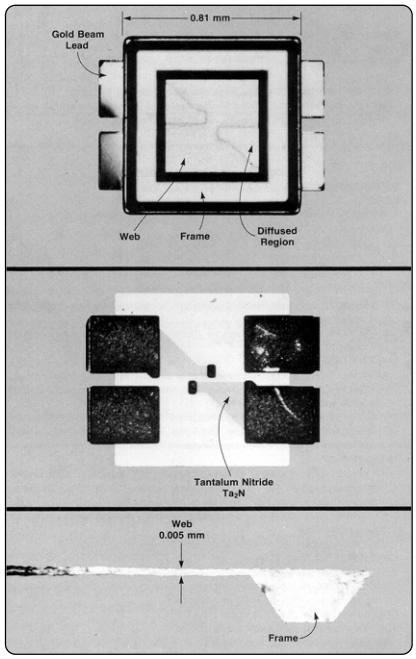

Figure 3-3. Photo-micrograph of the structure of the 8481A thermocouple chip on a thin silicon web.

Sometimes many pairs of junctions or thermocouples are connected in series and fabricated in such a way that the first junction of each pair is exposed to heat and the second is not. In this way the net emf produced by one thermocouple adds to that of the next, and the next, etc., yielding a larger thermoelectric output. Such a series connection of thermocouples is called a thermopile. Early thermocouples for sensing RF power were frequently constructed of the metals bismuth and antimony. To heat one junction in the presence of RF energy, the energy was dissipated in a resistor constructed of the metals making up the junction. The metallic resistor needed to be small in length and cross section to form a resistance high enough to be a suitable termination for a transmission line. Yet, the junction needed to produce a measurable change in temperature for the minimum power to be detected and measured. Thin-film techniques were normally used to build metallic thermocouples. These small metallic thermocouples tended to have parasitic reactances and low burnout levels. Further, larger thermopiles, which did have better sensitivity, tended to be plagued by reactive effects at microwave frequencies because the device dimensions became too large for good impedance match at higher microwave frequencies.

The thermocouple sensor

The modern thermocouple sensor was introduced in 1974[1] and is exemplified by the Agilent 8481A power sensor. It was designed to take advantage of both semiconductor and microwave thin-film technologies. The device, shown in Figure 3-3, consists of two thermocouples on a single integrated-circuit chip. The main mass of material is silicon.

The principal structural element is the frame made of p-type silicon, which supports a thin web of n-type silicon. The smoothly sloped sides of the frame result from an anisotropic etch acting on the silicon crystal planes. The thin web is produced by epitaxially growing it on the p-type substrate and then suitably controlling the etch, which also reveals the surface of the diffused regions in the web.

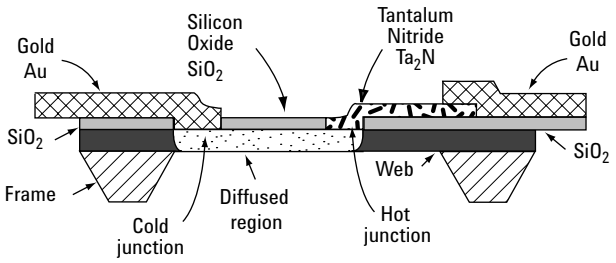

Figure 3-4. Cross section of one thermocouple. Power dissipated in the tantalum-nitride resistor heats the hot junction.

Figure 3-4 is a cross section through one of the thermocouples. One gold beam lead terminal penetrates the insulating silicon oxide surface layer to contact the web over the edge of the frame. This portion of the web has been more heavily doped by diffusing impurities into it. The connection between the gold lead and the diffused region is the cold junction of the thermocouple and the diffused silicon region is one leg of the thermocouple.

At the end of the diffused region near the center of the web, a second metal penetration to the web is made by a tantalum nitride film. This contact is the hot junction of the thermocouple. The tantalum nitride, which is deposited on the silicon oxide surface, continues to the edge of the frame where it contacts the opposite beam lead terminal. This tantalum nitride forms the other leg of the thermocouple.

The other edge of the resistor and the far edge of the silicon chip have gold beam-lead contacts. The beam leads not only make electrical contact to the external circuits, but also provide mounting surfaces for attaching the chip to a substrate, and serve as good thermal paths for conducting heat away from the chip. This tantalum-nitride resistor is not at all fragile in contrast to similar terminations constructed of highly conductive metals like bismuth/antimony.

As the resistor converts the RF energy into heat, the center of the chip, which is very thin, gets hotter than the outside edge for two reasons. First, the shape of the resistor causes the current density and the heat generated to be largest at the chip center. Second, the outside edges of the chip are thick and well cooled by conduction through the beam leads. Thus, there is a thermal gradient across the chip which gives rise to the thermoelectric emf. The hot junction is the resistor-silicon connection at the center of the chip. The cold junction is formed by the outside edges of the silicon chip between the gold and diffused silicon region.

The thin web is very important, because the thermocouple output is proportional to the temperature difference between the hot and cold junctions. In this case the web is fabricated to be 0.005 mm thick. Silicon is quite a good thermal conductor, so the web must be very thin if reasonable temperature differences are to be obtained from low power inputs.

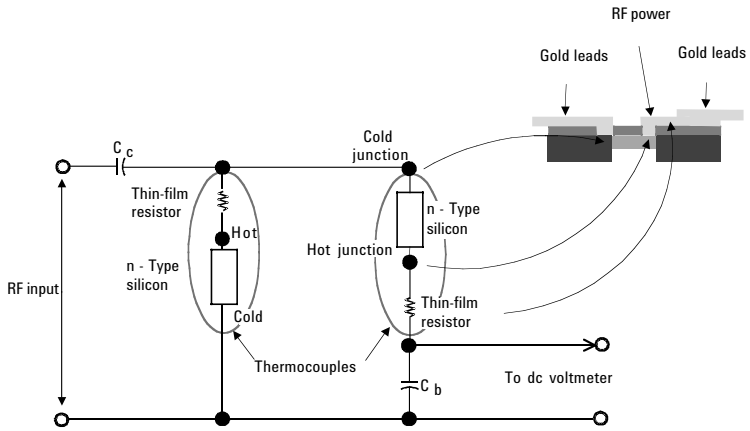

Figure 3-5. Schematic diagram of the 8481A thermocouple power sensor.

The 8481A power sensor contains two identical thermocouples on one chip, electrically connected as in Figure 3-5. The thermocouples are connected in series as far as the DC voltmeter is concerned. For the RF input frequencies, the two thermocouples are in parallel, being driven through coupling capacitor C_c. Half the RF current flows through each thermocouple. Each thin-film resistor and the silicon in series with it has a total resistance of 100 Ω. The two thermocouples in parallel form a 50 Ω termination to the RF transmission line.

The lower node of the left thermocouple is directly connected to ground and the lower node of the right thermocouple is at RF ground through bypass capacitor C_b. The DC voltages generated by the separate thermocouples add in series to form a higher DC output voltage. The principal advantage, however, of the two-thermocouple scheme is that both leads to the voltmeter are at RF ground; there is no need for an RF choke in the upper lead. If a choke were needed it would limit the frequency range of the sensor.

The thermocouple chip is attached to a transmission line deposited on a sapphire substrate as shown in Figure 3-6. A coplanar transmission line structure allows the typical 50 Ω line dimensions to taper down to the chip size, while still maintaining the same characteristic impedance in every cross-sectional plane. This structure contributes to the very low reflection coefficient of the Agilent 8480 Series sensors, its biggest contribution, over the entire 100 kHz to 50 GHz frequency range.

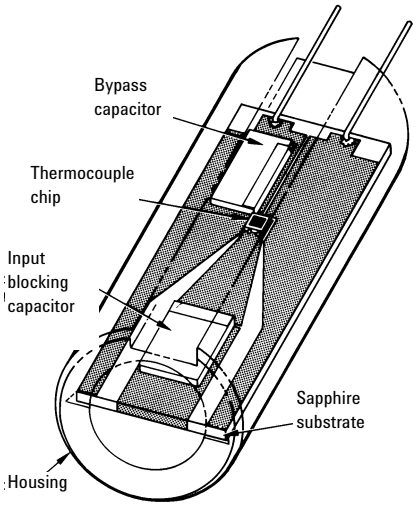

Figure 3-6. Sketch of the thermocouple assembly for the 8481A.

The principal characteristic of a thermocouple sensor for high frequency power measurement is its sensitivity in microvolts output per milliwatt of RF power input. The sensitivity is equal to the product of two other parameters of the thermocouple, the thermoelectric power and the thermal resistance.

The thermoelectric power (not really a power but physics texts use that term) is the thermocouple output in microvolts per degree Celsius of temperature difference between the hot and cold junction. In the 8481A thermocouple sensor, the thermoelectric power is designed to be 250μV/°C. This is managed by controlling the density of n-type impurities in the silicon chip.

The thickness of the 8481A silicon chip was selected so the thermocouple has a thermal resistance 0.4 °C/mW. Thus, the overall sensitivity of each thermocouple is 100 μV/mW. Two thermocouples in series, however, yield a sensitivity of only 160 μV/mW because of thermal coupling between the thermocouples; the cold junction of one thermocouple is heated somewhat by the resistor of the other thermocouple giving a somewhat smaller temperature gradient.

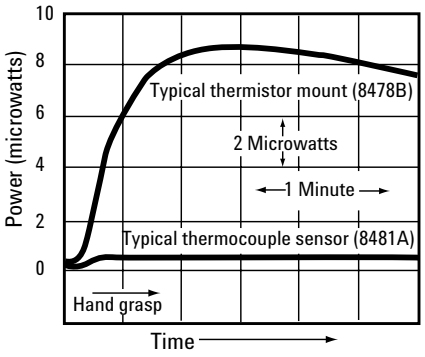

Figure 3-7. Zero drift of thermocouple and thermistor power sensors due to being grasped by a hand.

The thermoelectric voltage is almost constant with external temperature. It depends mainly on the temperature gradients and only slightly on the ambient temperature. Still, ambient temperature variations must be prevented from establishing gradients. The chip itself is only 0.8 mm long and is thermally short-circuited by the relatively massive sapphire substrate. The entire assembly is enclosed in a copper housing. Figure 3-7 depicts the superior thermal behavior of a thermocouple compared to a thermistor power sensor.

The thermoelectric output varies somewhat with temperature. At high powers, where the average thermocouple temperature is raised, the output voltage is larger than predicted by extrapolating data from low power levels. At a power level of 30 mW the output increases 3%, at 100 mW, it is about 10% higher. The circuitry in the power meters used with thermocouples compensates for this effect. Circuitry in the sensor itself compensates for changes in its ambient temperature.

The thermal path resistance limits the maximum power that can be dissipated. If the hot junction rises to 500 °C, differential thermal expansion causes the chip to fracture. Thus, the 8481A is limited to 300 mW maximum average power.

The thermal resistance combines with the thermal capacity to form the thermal time constant of 120 µs. This means that the thermocouple voltage falls to within 37% of its final value 120 µs after the RF power is removed. Response time for measurements, however, is usually much longer because it is limited by noise and filtering considerations in the voltmeter circuitry.

The only significant aging mechanism is thermal aging of the tantalum nitride resistors. A group of devices were stress tested, producing the results of Figure 3-8. These curves predict that if a device is stressed at 300 mW for 1 year, the resistance should increase by about 3.5%. Nine days at a half watt would cause an increase in resistance of 2%. On the other hand, aging effects of the tantalum-nitride termination are compensated by use of the power calibration procedure, whereby a precision 1 mW, 50 MHz source is used to set a known level on the meter.

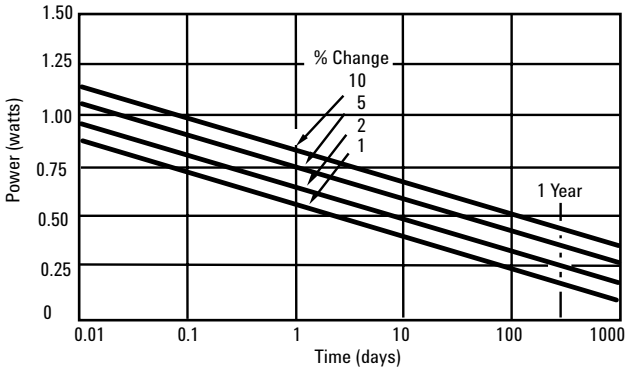

Figure 3-8. Results of a step stress aging test show percent change in thermocouple resistance when left at various power levels continuously for various periods of time.

It is relatively easy to adapt this sensor design for other requirements. For example, changing each tantalum-nitride resistor to a value of 150 Ω yields a 75 Ω system. To enhance low frequency RF performance, larger blocking and bypass capacitors extend input frequencies down to 100 kHz. This usually compromises high frequency performance due to increased loss and parasitic reactance of the capacitors. The Agilent 8482A power sensor is designed for 100 kHz to 4.2 GHz operation,while the standard 8481A operates from 10 MHz to 18 GHz.

Linearity characteristics for thermocouple and thermistor sensors

In the application of power sensors, there are two cases where the user would select sensors which exhibit the best detection linearity.

1. A measurement might involve using the linearity of the sensor itself to measure the linearity characteristic of some other component, such as an amplifier. This might be done by setting increasing power into the device under test, and monitoring the increase with a power sensor. In such a setup, the linearity of the sensor transfers directly to the measurement results.
2. Thermocouple sensors, as just described in this chapter, are "indirectly" calibrated by use of the 50 MHz, 1 mW reference source on the front panel of most Agilent power meters. This transfers that reference power to the sensor, but for all other powers, both higher and lower, the power readout depends on the linearity of the sensor. For thermocouple sensors, which depend on heating up the thermo-electric junctions, they are quite linear, and that characteristic is included in the basic power uncertainty specifications.

Recent research at the National Physical Laboratory in Teddington, UK, focused on characterizing the detection linearity of two types of sensors, thermistors and thermocouples.[6] Measurements were made on multiple sensors in each class, and are shown in Figure 3-9 and 3-10.

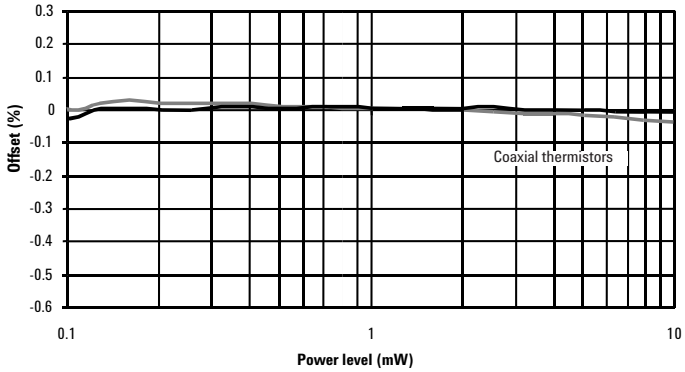

Data courtesy of NPL, Teddington, UK.

Figure 3-9. Mean linearity of seven units of model 8478A coaxial thermistor sensors from 0.1 to 10 mW. (8478A is an older model, the current model is 8478B.)

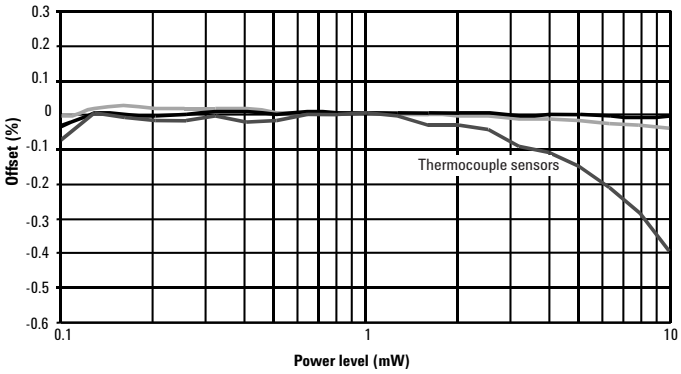

Data courtesy of NPL, Teddington, UK.

Figure 3-10. Mean linearity of four units of model 8481A coaxial thermocouple sensors from 0.1 to 10 mW.

The results seem reasonable, considering the technology involved. In the case of thermistor sensors, the DC-substitution process keeps the tiny bead of thermistor, at a constant temperature, backing off bias power as RF power is added. In the case of thermocouple sensors, as power is added, the detection microcircuit substrate with its terminating resistor runs at higher temperatures as the RF power increases. This naturally induces minor deviations in the detection characteristic. Linearity uncertainty for sensors is also treated in *Fundamentals Part 3*, and generally specified on product data sheets.

Power meters for thermocouple sensors

Introduction of thermocouple sensor technology required design of a new power meter architecture that could take advantage of increased power sensitivity, yet be able to deal with the very low output voltages of the sensors. This led to a family of power meter instrumentation starting with the 435A analog power meter, to the 436A digital power meter.[2, 3, 4, 5] Some years later the dual-channel 438A was introduced, which provided for computation of power ratios of channels A and B as well as power differences of channels A and B. The most recent Agilent 437B power meter offered digital data manipulations with the ability to store and recall sensor calibration factor data for up to ten different power sensors. All of those models have been replaced.

To understand the principles of the instrument architecture, a very brief description will be given for the first-introduced thermocouple meter, the 435A analog power meter. This will be followed by an introduction of the newest power meters, Agilent's E4418B (single channel) and E4419B (dual channel) power meters. They will be completely described in Chapter IV, after a new wide-dynamic-range diode sensor is introduced. Two peak and average power meters are introduced in Chapter V, the Agilent E4416/17A meters.

Thermocouple sensor DC output is very low-level (approximately 160 nV for 1 microwatt applied power), so it is difficult to transmit in an ordinary flexible connection cable. This problem is multiplied if the user wants a long cable (25 feet and more) between the sensor and power meter. For this reason it was decided to include some low-level AC amplification circuitry inside the power sensor, so only relatively high-level signals appear on the cable.

One practical way to handle such tiny DC voltages is to "chop" them to form a square wave, then amplify them with an AC-coupled system. After appropriate amplification (some gain in the sensor, some in the meter), the signal is synchronously detected at the high-level AC. This produces a high-level DC signal that is then further processed to provide the measurement result. Figure 3-11 shows a simplified block diagram of the sensor/meter architecture.

Cabling considerations led to the decision to include the chopper and part of the first AC amplifier inside the power sensor. The chopper itself (Figure 3-12) uses field-effect transistor switches that are in intimate thermal contact. It is essential to keep the two FET's at exactly the same temperature to minimize drift. To eliminate undesired thermocouple effects (in circuitry external to the RF sensor thermocouples), only one metal, gold, is used throughout the entire DC path. All these contributions were necessary to help achieve the low drift already shown in Figure 3-7.

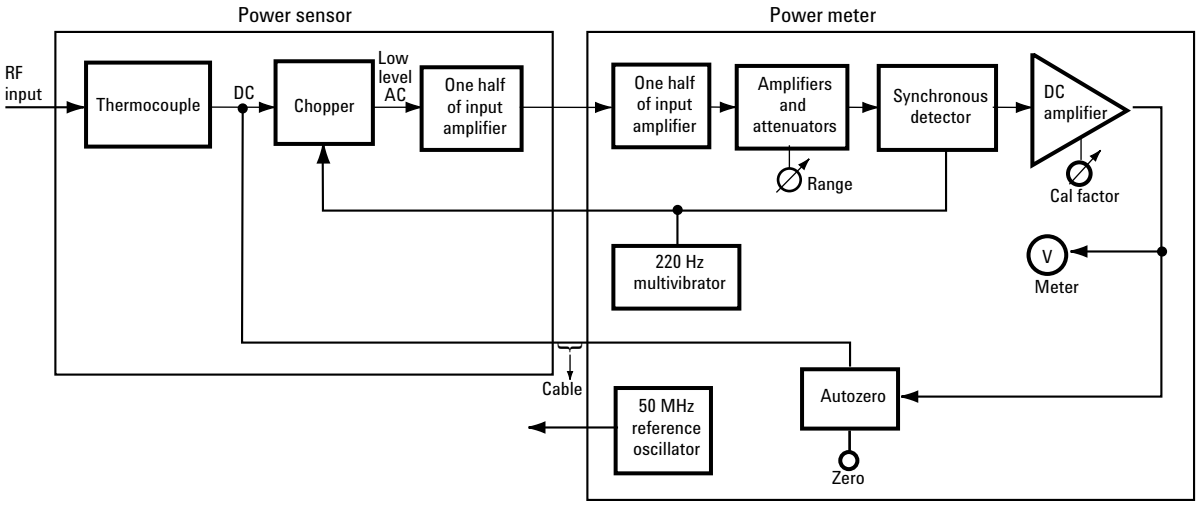

Figure 3-11. Basic power meter and thermocouple sensor block diagram.

The chopping frequency of 220 Hz was chosen as a result of several factors. Factors that dictate a high chopping frequency include lower 1/f noise and a larger possible bandwidth, and thereby faster step response. Limiting the chopping to a low frequency is the fact that small transition spikes from chopping inevitably get included with the main signal. These spikes are at just the proper rate to be integrated by the synchronous detector and masquerade as valid signals. The fewer spikes per second, the smaller this masquerading signal. However, since the spikes are also present during the zero-setting operation, and remain the same value during the measurement of a signal, the spikes are essentially removed from the meter indication by zerosetting and cause no error. The spikes do, however, use up dynamic range of the amplifiers.

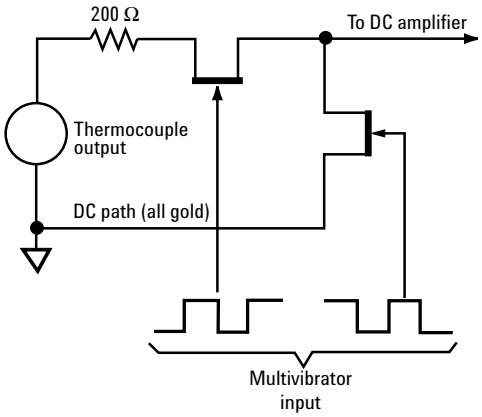

Figure 3-12. Simplified schematic of chopper amplifier.

One way to minimize noise while amplifying small signals is to limit the channel bandwidth. Since the noise generating mechanisms are broadband, limiting the amplifier bandwidth reduces the total noise power. The narrowest bandwidth is chosen for the weakest signals and the most sensitive range. As the power meter is switched to higher ranges, the bandwidth increases so that measurements can be made more rapidly. On the most sensitive range, the time constant is roughly 2 seconds, while on the higher ranges, the time constant is 0.1 seconds. A 2-second time constant corresponds to a 0 to 99% rise time of about 10 seconds.

Traceable power reference oscillator

An inherent characteristic of thermocouple power measurements is that such measurements are open-loop, and thus thermistor power measurements are inherently more accurate because of their DC-substitution, closed-loop process. The bridge feedback of substituted DC power compensates for differences between thermistor mounts and for drift in the thermistor resistance-power characteristic without recalibration.

With thermocouples, where there is no direct power substitution, sensitivity differences between sensors or drift in the sensitivity due to aging or temperature can result in a different DC output voltage for the same RF power. Because there is no feedback to correct for different sensitivities, measurements with thermocouple sensors are said to be open-loop.

Agilent thermocouple power meters solve this need for sensitivity calibration by incorporating a 50 MHz power-reference oscillator whose output power is controlled with great precision (±0.4%). To verify the accuracy of the system, or adjust for a sensor of different sensitivity, the user connects the thermocouple sensor to the power reference output and, using a calibration adjustment, sets the meter to read 1.00 mW. By applying the 1 mW reference oscillator to the sensor's input port just like the RF to be measured, the same capacitors, conductors and amplifier chain are used in the same way for measurement as for the reference calibration. This feature provides confidence in a traceability back to company and NMI standards.

Note: The calculation of the uncertainty budget, including the 50 MHz power reference, is covered in greater detail in *Fundamentals Part 3*. It should also be noted that Agilent has recently made improvements in the specifications of the 50 MHz reference oscillator.

The previous specification has been improved in the following areas. It is now "factory set to ±0.4% and traceable to the National Physical Laboratory of the UK." Expansion of the operating specification includes the following aging characteristics, which are now valid for 2 years:

Accuracy: (for 2 years)
±0.5% (23 ±3 °C)
±0.6% (25 ±10 °C)
±0.9% (0 - 55 °C)

Since the reference oscillator represents a reasonably large portion of the ultimate power measurement uncertainty budget, the smaller accuracy numbers in the specification leads to a lower overall measurement uncertainty. Another positive note is that the meters require less downtime in the calibration lab, now having a 2-year calibration cycle.

Figure 3-13. E4418B features many user-conveniences and a 90 dB dynamic measurement range. The 50 MHz, 1 mW reference output connector is at the top-right.

EPM Series power meters

The two-decade industry acceptance of thermocouple (and diode) sensor technology for RF power measurements has resulted in tens of thousands of units in the installed base around the world. Yet new technologies now allow for design of diode sensors with far larger dynamic range and new power meters with dramatically-expanded user features.

The E4418B (single channel) and E4419B (dual channel) power meters offer some significant user features:

- Menu-driven user interface, with softkeys for flexibility.
- Dedicated hardkeys for frequently used functions, such as Zero and Cal.
- Large LCD display for ease of reading.
- Built for wide-dynamic-range E-Series CW and average power sensors.
- Backward compatible with all 8480 Series sensors (except the discontinued 8484A).
- Fast measurement speed, up to 200 readings per second via the GPIB.
- Form, fit, function replacement with 437B and 438A power meters (preserves automation software code). See Chapter IV.

Since the meters provide more powerful measurement capability when teamed with the E-Series CW and average wide-dynamic range diode sensors, the detailed description of the meters will be presented in Chapter IV. This will first allow for a presentation of the technology for the new diode sensors with the range from –70 to +20 dBm, and then the meters that take advantage of this increased capability.

Conclusion

Because of their inherent ability to sense power with true square-law characteristics, thermocouple sensors are best suited for handling signals with complex modulations or multiple tones. They always respond to the true average power of a signal, modulation, and multiple signals. They are rugged, stable, and reliable.

The large installed worldwide base of Agilent thermocouple and diode sensors and their compatible power meters argues that any new power meters be designed to be backward compatible with older sensors. All current 8480 Series sensors will work with the EPM and EPM-P Series power meters. The newer E-Series sensors are not backwards-compatible with Agilent's older meters due to a modified interface design, which allows for download of EEPROM-stored constants.

Thermocouple sensors are based on a stable technology that will be used to measure RF power in many applications for a long time in the future.

[1] W.H. Jackson, "A Thin-Film Semiconductor Thermocouple for Microwave Power Measurements," Hewlett-Packard Journal, Vol. 26, No. 1 (Sept., 1974).
[2] A.P. Edwards, "Digital Power Meter Offers Improved Accuracy, Hands-Off Operation, Systems Capability," Hewlett-Packard Journal, Vol. 27 No. 2 (Oct. 1975).
[3] J.C. Lamy, "Microelectronics Enhance Thermocouple Power Measurements," Hewlett-Packard Journal, Vol. 26, No. 1 (Sept., 1974).
[4] "Power Meter-New Designs Add Accuracy and Convenience." *Microwaves*, Vol. 13, No. 11 (Nov., 1974).
[5] R.E. Pratt, "Very-Low-Level Microwave Power Measurements," Hewlett-Packard Journal, Vol. 27, No. 2 (Oct., 1975).
[6] Holland, K., and Howes, J., "Improvements to the Microwave Mixer and Power Sensor Linearity Measurement Capability at the National Physical Laboratory," (Teddington, UK) IEE Proc.-Sci Meas. Technology, Nov. 2002.

IV. Diode Sensors and Instrumentation

Rectifying diodes have long been used as detectors and for relative power measurements at microwave frequencies. The earliest diodes were used mostly for envelope detection and as nonlinear mixer components in super-heterodyne receivers. For absolute power measurement, however, diode technology had been limited mainly to RF and low microwave frequencies.

High-frequency diodes began with point-contact technology which evolved from the galena crystal and cat-whisker types of early radio and found application as early as 1904.[1] Point-contact diodes were extremely fragile, not very repeatable, and subject to change with time. It was the low-barrier Schottky (LBS) diode technology that made it possible to construct diodes with metal-semiconductor junctions for microwave frequencies that were very rugged and consistent from diode to diode. These diodes, introduced as power sensors in 1974, were able to detect and measure power as low as –70 dBm (100 pW) at frequencies up to 18 GHz.[2]

This chapter will review the semiconductor principles as they apply to microwave detection, briefly review LBS technology and then describe the latest planar-doped-barrier (PDB) diode technology. It will describe how such devices are designed into power sensor configurations and introduce a new CW-diode sensor with an impressive 90 dB dynamic power range using digital-detection-curve correction techniques. Then, a novel two-path diode sensor with wide dynamic range is discussed. Signal and waveform effects for non-CW signals operating above the square-law range will also be examined.

The EPM Series power meters will be described, which exploit the advantages of the new 90-dB-range sensors and offer major user-conveniences as well.

Principles of diode detectors

Diodes convert AC signals to DC by way of their rectification proper-ties, which arise from their nonlinear current-voltage (i-v) characteristic. It might seem that an ordinary silicon p-n junction diode would, when suitably packaged, be a sensitive RF detector. However, stored charge effects limit the bandwidth of the p-n junction. The Schottky[1] barrier diode does not store charge in its junction but most of them have extremely high impedance at low signal levels. A RF signal in the rage of –20 dBm is required to overcome the 0.3-volt junction voltage of a conventional Schottky diode. One alternative is to bias the diode to 0.3 V and is a usable approach if the detected output can be AC coupled with eliminates the drift introduced by the bias. With AC coupling, the minimum power that can be metered by a biased diode may be improved by about 10 dB due to the drift and noise introduced by bias current. A typical application for this technique would be the diode detectors used for scalar network analyzers.

Metal-semiconductor junctions, exemplified by point-contact technology, exhibit a low potential barrier across their junction, with a forward voltage of about 0.3 V. They have superior RF and microwave performance, and were popular in earlier decades. LBS diodes, which are metal-semiconductor junctions, succeeded point-contacts and vastly improved the repeatability and reliability. Figure 4-1 shows a typical diode i-v characteristic of an LBS junction, expanded around the zero-axis to show the square-law (see below) region.

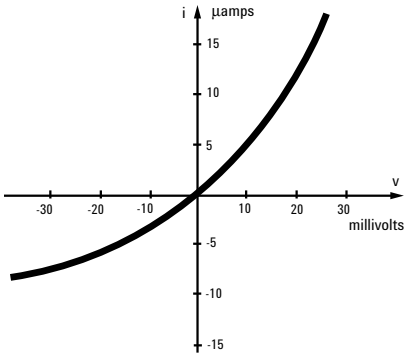

Figure 4-1. The junction rectifying characteristic of a low-barrier Schottky diode, showing the small-signal, square-law characteristic around the origin.

1. The diode metal-semiconductor junction rectifying effect was named for physicist Walter Schottky (1886-1976) who advanced the theory for the process.

Mathematically, a detecting diode obeys the diode equation

$$i = I_S (e^{\alpha v} - 1) \qquad \text{(Equation 4-1)}$$

where $\alpha = q/nKT$, and i is the diode current, v is the net voltage across the diode, I_S is the saturation current and is constant at a given temperature. K is Boltzmann's constant, T is absolute temperature, q is the charge of an electron and n is a correction constant to fit experimental data (n equals approximately 1.1 for the devices used here for sensing power). The value of α is typically a little under 40 $(v)^{-1}$, in this case approximately 36 v^{-1}.

Equation 4-1 is often written as a power series to better analyze the rectifying action,

$$i = I_s \left(\alpha v + \frac{(\alpha v)^2}{2!} + \frac{(\alpha v)^3}{3!} + \cdots\right) \qquad \text{(Equation 4-2)}$$

It is the second and other even-order terms of this series which provide the rectification. For small signals, only the second-order term is significant so the diode is said to be operating in the square-law region. In that region, output i (and output v) is proportional to RF input voltage squared. When v is so high that the fourth and higher order terms become significant the diode response is no longer in the square law region. It then rectifies according to a quasi-square-law i-v region which is sometimes called the transition region. Above that range it moves into the linear detection region (output v proportional to input v).

For a typical packaged diode, the square-law detection region exists from the noise level up to approximately –20 dBm. The transition region ranges from approximately –20 to 0 dBm input power, while the linear detection region extends above approximately 0 dBm. Zero dBm RF input voltage is equivalent to approximately 220 mV (rms) in a 50 Ω system. For wide-dynamic-range power sensors, it is crucial to have a well-characterized expression of the transition and linear detection range.

Figure 4-2 shows a typical detection curve, starting near the noise level of –70 dBm and extending up to +20 dBm. It is divided up into the square law, transition and linear regions. (Noise is assumed to be zero to show the square-law curve extends theoretically to infinitely small power.) Detection diodes can now be fabricated which exhibit transfer characteristics that are highly stable with time and temperature. Building on those stable features, data correction and compensation techniques can take advantage of the entire 90 dB of power detection range.

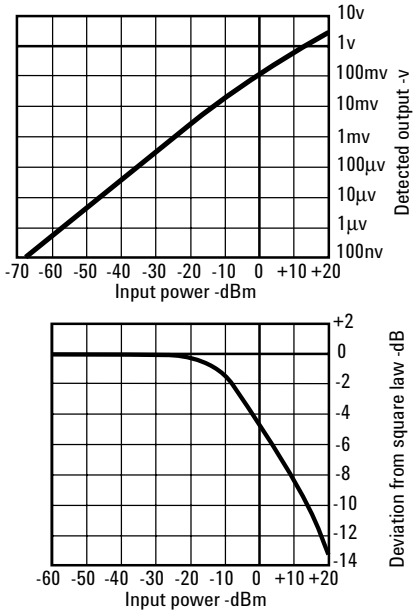

Figure 4-2. The diode detection characteristic ranges from square law through a transition region to linear detection.

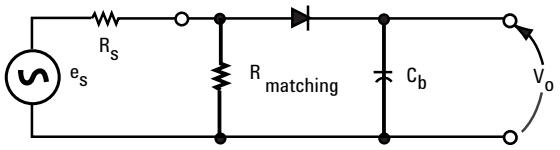

Figure 4-3. Circuit diagram of a source and a diode detector with matching resistor.

The simplified circuit of Figure 4-3 represents an unbiased diode device for detecting low level RF signals. Detection occurs because the diode has a nonlinear i-v characteristic; the RF voltage across the diode is rectified and a DC output voltage results.

If the diode resistance for RF signals were matched to the generator source resistance, maximum RF power would be delivered to the diode. However, as long as the RF voltage is impressed across the diode, it will detect RF voltage efficiently. For reasons explained below, diode resistance for small RF signals is typically much larger than 50 Ω and a separate matching resistor is used to set the power sensor's input termination impedance. Maximum power is transferred to the diode when the diode resistance for small RF voltages is matched to the source resistance. The diode resistance at the origin, found by differentiating Equation 4-1, is:

$$R_o = \frac{1}{\alpha I_s} \qquad \text{(Equation 4-3)}$$

Resistance R_o is a strong function of temperature which means the diode sensitivity and the reflection coefficient are also strong functions of temperature. To achieve less temperature dependence, R_o is much larger than the source resistance and a 50 Ω matching resistor serves as the primary termination of the generator. If R_o of the diode of Figure 4-3 were made too large, however, there would be poor power conversion from RF to DC; thus, a larger R_o decreases sensitivity. An origin resistance of 1–2 kΩ will be obtained with diodes having a reverse saturation current (I_s) of between 27.5 to 13.8 µA. A compromise between good sensitivity to small signals and good temperature performance results from making I_s about 10 microamps and R_o approximately 2.75 kΩ.

The desired value of saturation current, I_s, can be achieved by constructing the diode of suitable materials that have a low potential barrier across the junction. Schottky metal-semiconductor junctions can be designed for such a low-barrier potential.

The origin resistance R_o is a very useful concept in understanding how a detector diode will operate under a wide variety of conditions. It forms the real part of the source impedance of the detected output, so the effect of finite load resistance can be estimated. If the value of the RF bypass capacitor, C_b, is known, the overall risetime may be accurately estimated. If the variation in I_s versus temperature (Silicon LBSD's double every 10 ˚C rise) is considered, the temperature coefficient of the loaded detector can also be estimated.

Of course, R_o is also sensitive to the input power into the device, and can only be considered to be constant for junction voltages which are lower than the "thermal voltage" V_t=nKT/q, or about 28 mV peak. This limit correlates well with the power level where the output departs from square law response in a 50 Ω system.

Using diodes for sensing power

Precision semiconductor fabrication processes for silicon allowed the Schottky diodes to achieve excellent repeatability and, because the junction area was larger, they were more rugged. Agilent's first use of such a low-barrier Schottky diode (LBSD) for power sensing was introduced in 1975 as the 8484A power sensor.[2] It achieved an exceptional power range from –70 (100 pW) to –20 dBm (10 µW) from 10 MHz to 18 GHz.

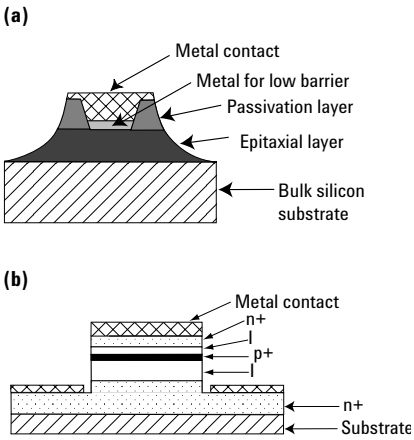

Figure 4-4. Idealized cross sections of two diode configurations. (a) low-barrier Schottky. (b) planar-doped-barrier.

As Gallium-Arsenide (GaAs) semiconductor material technology advanced in the 1980s, such devices exhibited superior performance over silicon in the microwave frequencies. A sophisticated diode fabrication process known as planar-doped-barrier (PDB) technology offered real advantages for power detection.[3] It relied on a materials preparation process called molecular beam epitaxy for growing very thin epitaxial layers. Figure 4-4 shows the device cross sections of the two types of diode junctions, low-barrier Schottky (Figure 4-4(a)) and planar-doped barrier (Figure 4-4(b)) diodes. The doping profile of the PDB device is n+ –I–p+–I–n+, with intrinsic layers spaced between the n+ and p+ regions. The i/v characteristic has a high degree of symmetry which is related to the symmetry of the dopants.

The p^+ region is fabricated between the two intrinsic layers of unequal thickness. This asymmetry is necessary to give the PDB device the characteristics of a rectifying diode. An important feature of the PDB diode is that the device can be designed to give a junction capacitance, C_o, that is both extremely small (20 fF or less) (femto Farad) and nearly independent of the bias voltage. C_o is also independent of the size of the metal contact pad.

As a result of the very stable C_o versus bias voltage, the square-law characteristics of this device versus frequency are significantly more constant than those of metal-to-semiconductor devices. Low capacitance coupled with low junction resistance allows excellent microwave signal performance since the low junction resistance lowers the radio correction (RC) time constant of the junction and raises the diode cutoff frequency.

A PDB diode is far less frequency-sensitive than a normal p-n junction diode because of the intrinsic layer at the junction.[4] In a p-n junction diode the equivalent capacitance of the junction changes with power level, but in the planar-doped-barrier diode, junction capacitance is determined by the intrinsic layer, which remains almost constant as a function of power.

Agilent uses a specialized integrated circuit process that allows custom tailoring of the doping to control the height of the Schottky barrier. This controlled doping makes it practical to operate the detector diode in the current mode, while keeping the video resistance low enough to maintain high sensitivity.

The first power sensor application for PDB diodes was the Agilent 8481/85/87D Series power sensors, introduced in 1987.[4] The 8481D functionally replaced the low-barrier-Schottky 8484A sensor. The new PDB sensor employed two diodes, fabricated on the same chip using microwave monolithic integrated circuit (MMIC) chip technology. The two diodes were deposited symmetrically about the center of a coplanar transmission line and driven in a push-pull manner for improved signal detection and cancellation of common-mode noise and thermal effects. This configuration features several advantages:

- Thermoelectric voltages resulting from the joining of dissimilar metals, a serious problem below –60 dBm, are cancelled.
- Measurement errors caused by even-order harmonics in the input signal are suppressed due to the balanced configuration.
- A signal-to-noise improvement of 1 to 2 dB is realized by having two diodes. The detected output signal is doubled in voltage (quadrupled in power) while the noise output is doubled in power since the dominant noise sources are uncorrelated.
- PDB devices also have higher resistance to electrostatic discharge and are more rugged than Schottky's.
- Common-mode noise or interference riding on the ground plane is cancelled at the detector output. This is not RF noise but metallic connection noises on the meter side.

PDB diode technology provides some 3000 times (35 dB) more efficient RF-to-DC conversion compared to the thermocouple sensors of Chapter III.

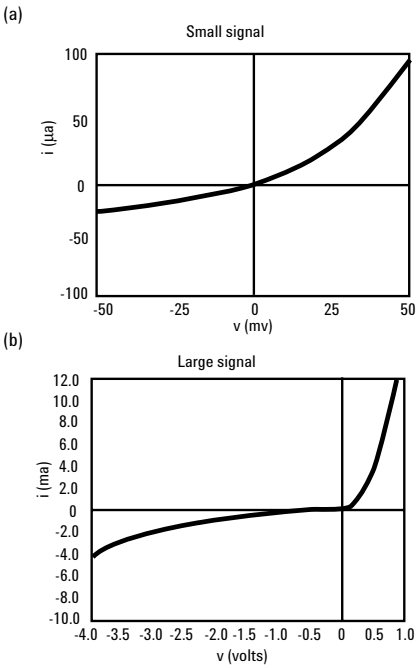

Figure 4-5. The i-v characteristics of a PDB diode are shown for two different drive voltage regions. The assymetry of the p^+ layer can be used to modify the shape of the i-v curve, while not affecting some of the other diode parameters such as C_0 and R_0.

Figure 4-5 shows two regions of the i-v characteristic of a typical PDB diode. Figure 4-5(a) shows the small signal region, while Figure 4-5(b) shows the larger signal characteristics to include the linear region as well as the breakdown region on the left.

They also provide accurate square-law performance from –70 to –20 dBm. Diode sensor technology excels in sensitivity, although realistically, thermocouple sensors maintain their one primary advantage as pure square-law detectors for the higher power ranges of –30 to +20 dBm. Hence neither technology replaces the other and the user's measuring application determines the choice of sensors.

In detecting power levels of 100 pW (70 dBm) the diode detector output is about 50 nanovolts. This low signal level requires sophisticated amplifier and chopper circuit design to prevent leakage signals and thermocouple effects from dominating the desired signal. Earlier diode power sensors required additional size and weight to achieve controlled thermal isolation of the diode. The dual-diode configuration balances many of the temperature effects of those highly-sensitive circuits and achieves superior drift characteristics in a smaller, lower-cost structure.

Wide-dynamic-range, CW-only power sensors

Digital signal processing and microwave semiconductor technology have now advanced to the point where dramatically improved performance and capabilities are available for diode power sensing and metering. New diode power sensors are now capable of measuring over a dynamic power range of –70 to +20 dBm, an impressive range of 90 dB. This permits the new sensors to be used for CW applications which previously required two separate sensors.

The E4412A power sensor features a frequency range from 10 MHz to 18 GHz. The E4413A power sensor operates to 26.5 GHz (Option H33 extends the range to 33 GHz). Both provide the same –70 to +20 dBm power range. A simplified schematic of the new sensors is shown in Figure 4-6. The front end construction is based on MMIC technology and combines the matching input pad, balanced PDB diodes, FET choppers, integrated RF filter capacitors, and the line-driving pre-amplifier. All of those components operate at such low signal levels that it was necessary to integrate them into a single thermal space on a surface-mount-technology PC board.

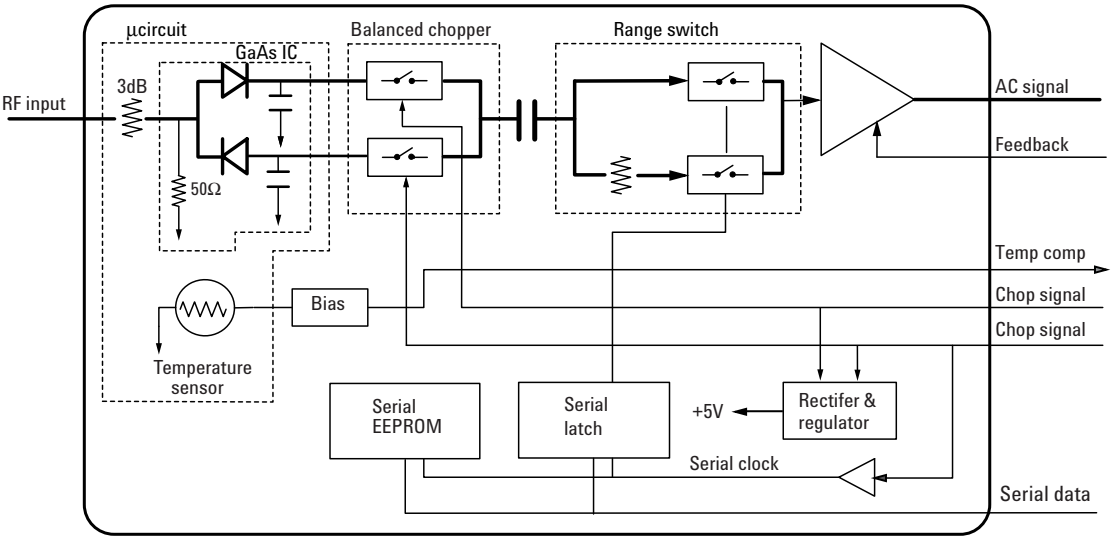

Figure 4-6. Simplified schematic for the E4412/13A power sensors. The 90 dB power range is achieved using data stored in the individual sensor EEPROM which contains linearization, temperature compensation and calibration factor corrections.

To achieve the expanded dynamic range of 90 dB, the sensor/meter architecture depends on a data compensation algorithm that is calibrated and stored in an individual EEPROM in each sensor. The data algorithm stores information of three parameters, input power level vs frequency vs temperature for the range 10 MHz to 18 or 26.5 GHz and –70 to +20 dBm and 0 to 55 °C.

At the time of sensor power-up, the power meter interrogates the attached sensor using an industry-standard serial bus format, and in turn the meter receives the upload of sensor calibration data. An internal temperature sensor supplies the diode's temperature data for the temperature-compensation algorithm in the power meter.

Since the calibration factor correction data will seldom be used manually, it is no longer listed on the sensor label of the E-Series sensors. The data is always uploaded into the power meter on power-up or when a new sensor is connected. The new sensors store cal factor tables for two different input power levels to improve accuracy of the correction routines. If the cal factor changes upon repair or recalibration, the new values are re-loaded into the sensor EEPROM. For system users who need the cal factor for program writing, the data is furnished on a calibration certificate.

Wide-dynamic-range average power sensors

Today's average power measurement needs, as highlighted by complex digital modulation formats such as code division multiple access (CDMA), are for accurate measurements in the presence of high crest factors (peak-to-average ratio), and often require a dynamic range greater than 50 dB. As the Agilent E4412A and E4413A sensors are designed to measure the average power of CW signals, they cannot satisfy this requirement.

Agilent's approach to creating a wide-dynamic-range, average power sensor to meet this need is based on a dual sensor, diode pair/attenuator/diode pair topology as proposed by Szente et. al. in 1990.[5] This topology has the advantage of always maintaining the sensing diodes within their square law region and therefore will respond properly to complex modulation formats as long as the sensor's correct range is selected.

This approach was further refined by incorporating diode stacks in place of single diodes to extend square law operation to higher power levels at the expense of sensitivity. A series connection of m diodes results in a sensitivity degradation of 10 log(m) dB and an extension upwards in power limits of the square law region maximum power of 20 log(m) dB, yielding a net improvement in square law dynamic range of 10 log(m) dB compared to a single diode detector.

The Agilent E-Series E9300 power sensors are implemented as a modified barrier integrated diode (MBID)[6] with a two diode stack pair for the low power path (–60 to –10 dBm), a resistive divider attenuator and a five diode stack pair for the high power path (–10 to +20 dBm), as shown in Figures 4-7(a) and 4-7(b). Additionally, series FET switches are used off-chip to allow the low path diodes to self-bias off when not in use.

(a)

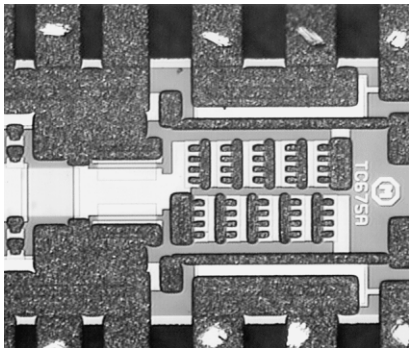

(b) **Resistive power splitter**

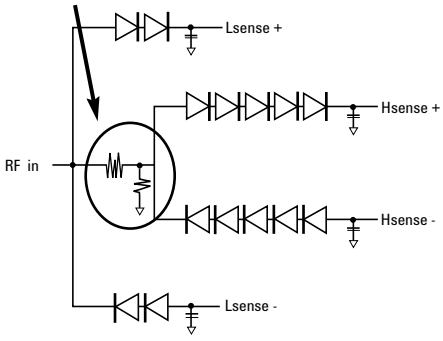

Figure 4-7 (a) Photograph of MBID. (b) Schematic of MBID.

Typical deviation from square law for the low power path (–60 to –10 dBm) and high power path (–10 to +20 dBm) for the E-Series E9300 power sensors is shown in Figure 4-8.

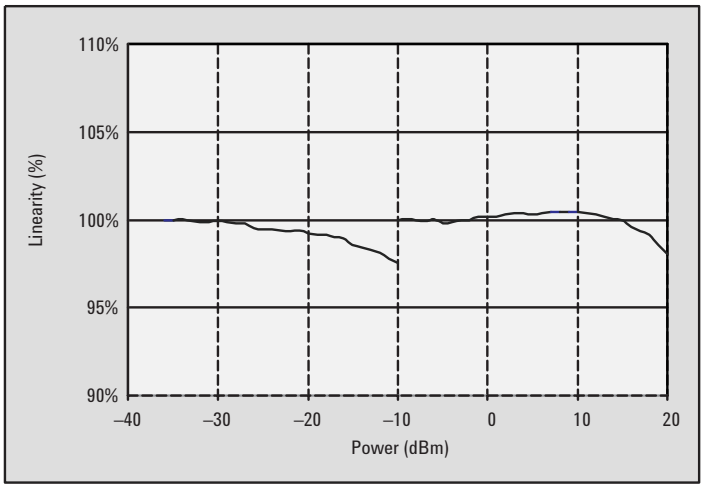

Figure 4-8. E9300 power sensor linearity. The linearity at the –10 dBm switching point is specified as being typically ≤ ±0.5% (≤ ±0.02 dB). The E9300 power sensors switch quickly and automatically between ranges, providing a transparent 80 dB dynamic range.

The decision for switching between the low and high power paths is made on the basis of the average power detected by the meter. For example, a –12 dBm average power signal with a high crest factor (peak-to-average ratio) would be measured by the low power path. For most CDMA signals, such as IS-95A, E9300 sensors will give better than ±0.05 dB accuracy up to –10 dBm average power using the low power path. However, for some 3G CDMA signals, with aligned symbols that have almost 20 dB maximum peak-to-average ratio, the accuracy of the measurement during the high power crests would be compromised. This is due to the sensor being in the low power path and the diodes being operated well outside the square law region of the low power path during the crests. A Range Hold function for the high power path deals with this situation as it allows both the peak and average powers to be measured in the square law region of the high power path.

To avoid unnecessary switching when the power level is near –10 dBm, switching point hysteresis has been added. This hysteresis causes the low power path to remain selected as the power level is increased up to approximately –9.5 dBm, above this power the high power path is selected. The high power path remains selected until approximately –10.5 dBm is reached as the signal level decreases. Below this level the low power path is selected.

To provide user-meaningful sensor information relevant to the numerous power measurement scenarios, from a temperature controlled manufacturing or R&D environment to field installation and maintenance applications, warranted specifications for E9300 sensors are provided over the temperature ranges 25 ±10 °C as well as 0 to 55 °C. Also, supplemental information is provided at 25 °C to illustrate the typical performance achievable, as shown in Figure 4-9.

Power range	Linearity (25 ±10 °C)	Linearity (0 to 55 °C)
–60 to –10 dBm	± 3.0%	± 3.5%
–10 to 0 dBm	± 2.5%	± 3.0%
0 to +20 dBm	± 2.0%	± 2.5%

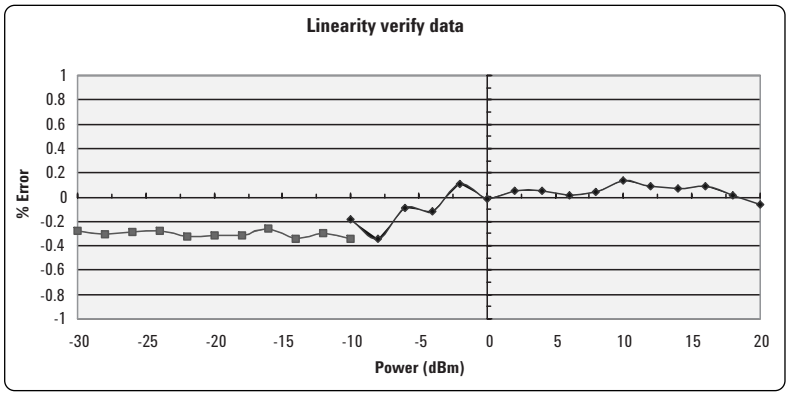

Power range	–30 to –20 dBm	–20 to –10 dBm	–10 to 0 dBm	0 to +10 dBm	+10 to +20 dBm
Measurement uncertainty	± 0.9%	± 0.8%	± 0.65%	± 0.55%	± 0.45%

Figure 4-9. Typical power linearity performance at 25 °C, after a zero and calibration, (top chart) along with the measurement uncertainty for different power ranges is shown (lower plot). By providing this type of specification data, users can better understand how the power sensor will perform for their particular application and environment and so allow informed sensor selection.

A versatile power meter to exploit the E-Series power sensors

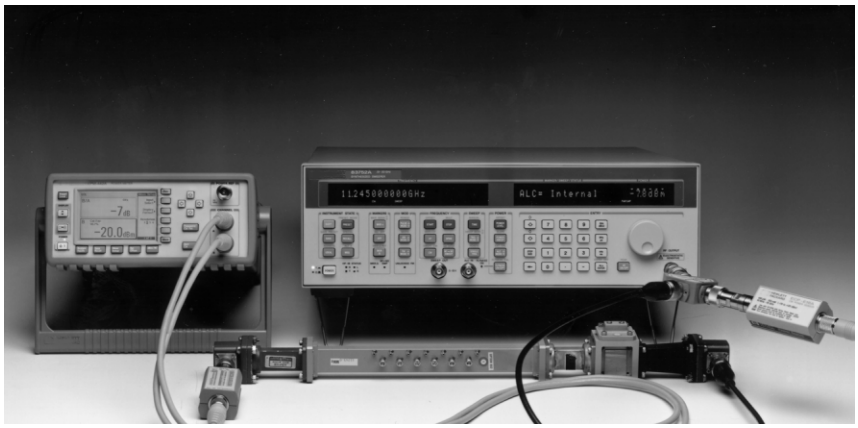

Figure 4-10. E4419B dual-channel power meter measures insertion loss of a 11.245 GHz waveguide bandpass filter, using the meter's power ratio mode, plus a sweeper and power splitter. Agilent's 90 dB dynamic-range sensors are ideal for such high-attenuation measurements.

Two power meters, E4418B (single channel) and E4419B (dual channel) take advantage of the sensor's 90 dB power measuring range. More importantly, advances in digital signal processing (DSP) technology now provide significant increases in measurement speeds. Digital processing permits functional conveniences resulting in a dramatically more versatile power meter.

The basic meter architecture is based on DSP technology that improves performance by removing meter range switching and their delays (except for a single range-switching transition point). It also provides faster signal detection. The DSP module performs several other functions, synchronous detection (de-chopping), matches up the two analog-to-digital converter (ADC) channels, and does the programmable filtering. It provides a 32-bit digital number that is proportional to the detected diode voltage over a 50 dB power range.

The power meter uses the uploaded calibration data from each connected sensor to compensate for the three critical sensor parameters, power from –70 to +20 dBm, frequency for its specified band, and operating temperature.

The calibration routine requiring connection to the 50 MHz power reference furnishes the power traceability path for the sensor connected. The operator then keys in the frequency of the RF signal under test so that the meter corrects for the sensor calibration factor. Mismatch uncertainty must still be externally calculated because the reflection coefficient of the unknown power source is usually not available.

Figure 4-11 shows a simplified schematic of the E4418B meter (see Figure 4-6 for reference to the associated E-Series sensors). The pre-amplified sensor output signal receives some early amplification, followed by some signal conditioning and filtering. The signal then splits, with one path receiving amplification. Both low and high-level chopped signals are applied to a dual ADC. A serial output from the ADC takes the sampled signals to the digital signal processor that is controlled by the main microprocessor. A differential drive signal, synchronized to the ADC sampling clock, is output to the sensor for its chopping function.

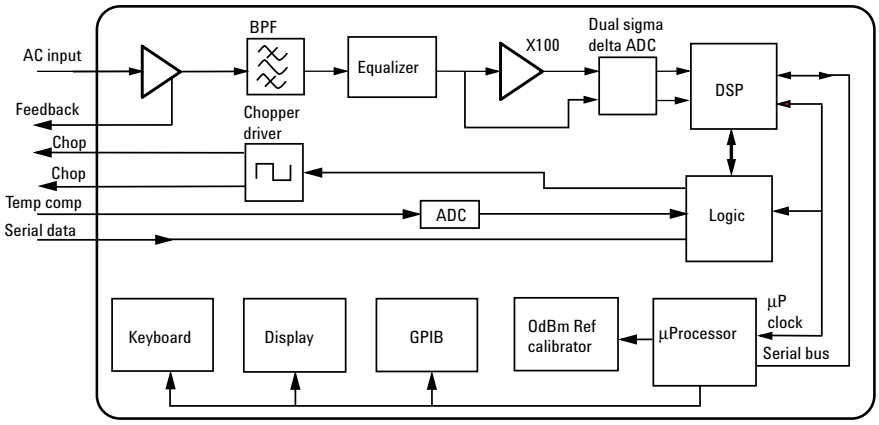

Figure 4-11. Simplified schematic of E4418B shows the transition to digital signal processing (DSP) architecture.

The dual-sigma-delta ADC provides a 20-bit data stream to the digital signal processor, which is under control of the main microprocessor. There is no range switching as in traditional power meters which maintain an analog signal path. Even the synchronous detection is performed by the ADC and DSP rather than use of a traditional synchronous detector.

Computation power permits the user to manipulate the basic measurement data to get desired units or format. Power reads out in watts or dBm, and inputs may be keyed in to compensate for attenuators or directional coupler losses to the unknown signal in front of the power sensor. Cabling losses can be compensated by entering the loss as a digital offset value.

For the E4419B two-channel power meter, either input power or both may be displayed, or for certain applications power ratios A/B or B/A might be useful. For example, if the two power sensors are sampling forward and reverse power in a transmission line using a dual directional coupler, these ratios would yield power reflection coefficient. The power difference, A–B or B–A, can be used for other applications. For example, using a dual directional coupler to sample forward and reverse power in a line, the power difference is a measure of net forward power being absorbed by a device under test. This is quite important in testing devices with very high reflections, such as mixer diodes, which are often deliberately mis-matched for better noise figure.

Power changes are displayed with the relative power function. And although the main display is all digital, a simple "peaking" display simulates an analog meter pointer and allows a user to adjust a unit under test for maximizing power output.

In system applications, the new single-channel power meter, when used with the wide-dynamic-range sensors can achieve 200 measurements per second. The programming code is also designed to be backward compatible with the previous 437B (for programming applications, the E4419B is code compatible with the 438A). Of course, the new meter offers far more versatile programming functions too, to handle modern complex test procedures. However, old software can be re-used to make programming projects more efficient.

When old sensors are utilized with the new meter, the calibration factor vs. frequency table printed on the label of the sensor must be keyed into the new power meters to take the fullest advantage of the measurement accuracy. A table of frequencies vs. cal factor is displayed and the routine prompted by the softkey display to ease editing.

Potential users of the new power meters will find that specification listings for this DSP-architecture meter without range switching will not follow traditional power meter range specifications, yet the meter meets the same range performance as the 43X-Series meters.

Traceable power reference

All thermocouple and diode power sensors require a power reference to absolute power, traceable to the manufacturer or national standards. Power meters accomplish this power traceability by use of a highly stable, internal 50 MHz power reference oscillator. When used together, the 50 MHz reference and the sensor calibration factor data supplied with each sensor yields the lowest measurement uncertainty. All Agilent sensors are supplied with calibration factor versus frequency data. This includes both the value and uncertainty of each point.

The 1 mW reference power output is near the center of the dynamic range of thermocouple power sensors, but above the range of the sensitive diode sensor series. Therefore, a special 30 dB calibration attenuator, designed for excellent precision at 50 MHz, is supplied with each diode power sensor. When that attenuator is attached to the power reference output on the power meter, the emerging power is 1 µW (–30 dBm). The attenuator design is such that a maximum error of 1% is added to the calibration step. See Chapter III, for specification detail on the reference oscillator.

Signal waveform effects on the measurement uncertainty of diode sensors

Along with the great increase in measurement flexibility of the E4412/3A and E9300-Series power sensors, comes several new applications guidelines. These must be understood and followed to obtain valid measurement results when dealing with complex and non-CW signals. The Agilent EPM-P peak and average power meter and associated sensors are described next in Chapter V.

These guidelines distinguish between earlier diode sensors of the 8481D vintage and the E-Series CW-only diode sensors or the E9300-Series dual-path sensors.

The power range from approximately –20 to +20 dBm is above the square-law region, and one in which the Agilent EPM (or EPM-P, Chapter V) Series power meters use digital-diode-curve correction to provide accurate power measurement for pure CW signals all the way from –70 to +20 dBm. The EPM meters and companion E-Series sensors provide fully specified performance over that entire dynamic range of –70 to +20 dBm.

Since the unique design of the two-path E9300-Series sensors always keeps the diodes in their square-law range, they can accept non-CW signals across their specified power range, if the peak value remains below the maximum specified power.

The following explanation reviews the effects of complex signals on existing 8481D-type diode sensors for non-CW or complex modulation signals.

Some examples of complex (non-CW) signals are as follows: 1) Pulsed RF such as radar or navigation formats, 2) Two-tone or multiple-tone signals such as those that might be present in a telecommunications channel with multiple sub-channels, 3) AM signals that have modulation frequencies higher than the bandwidth of the power meter detection filtering (in the kHz range for the E4418B), 4) Digital-phase-shift-keyed (PSK) modulations, 5) quadrature amplitude modulation (QAM) modulated signals, and 6) Pulse-burst formats.

Here is a summary of the measurement guidelines for diode sensors:

1) Using the 8481D type diode power sensors, any complex signal will yield highly-accurate measurement results as long as the peak power levels of the unknown signal are maintained below –20 dBm. In addition, the lowest-frequency-component of any modulation frequency must be above approximately 500 Hz. Since the power range of the 8481D-type diode sensors are automatically restricted by Agilent power meters to a top level of –20 dBm, the user need only assure that no peak power levels go above –20 dBm.

When peak power levels exceed approximately –20 dBm, accurate measurements can be accomplished by the simple expedient of attenuating the unknown signal through an external precise fixed or step attenuator, such that the complex signal peak power does not exceed –20 dBm. If pulse modulation frequencies are near the power meter chopping rate of 220 Hz or multiples thereof, some meter “beats” may be observed.

2) Using the E4412/3A power sensors, pure-CW signals will yield accurate results across their entire –70 to +20 dBm dynamic range. One reason E-Series sensors may not be used for pulse power within their square-law range is that their output circuit filters are optimized for fast response to aid high data-rate automation.

3) Using the E9300-Series sensors, pulsed and complex-modulated signals will yield accurate results if peak powers remain below the maximum specified input power.

4) For non-CW signals with average powers between –20 and +20 dBm, use the thermocouple sensors for true average power sensing.

5) Peak and average sensor/meter technology, which is specifically designed for peak and complex modulations, is introduced in the next chapter.

Thermal sensors such as the thermocouple are pure square law because they convert the unknown RF power to heat and detect that heat transfer. Conversely, it is less easy to understand how diode sensors can perform the square-law function without the heat transfer step in the middle. Diode detectors do deliver pure square-law performance in their lower power ranges below –20 dBm due to their mathematical detection transfer function as described by the power series Equation 4-2.

A two-tone example might clarify the measurement example. Consider two CW signals, f_1 and f_2 , of power level 0 dBm (1 mW) each, and separated by 1 MHz. In a 50 Ω system, each carrier would have voltage magnitudes of $v_1 = v_2 =$ 0.223 V (rms). If the two-tone signal were measured by an 8481A thermocouple sensor, each carrier would convert the 1 mW into heat for a total of 2 mW.

Using a voltage vector analysis, these two-tone signals would be represented by a voltage minimum of zero and a voltage maximum of 0.446 V occurring at a frequency of 1 MHz. The problem then becomes evident when one realizes that two times voltage represents four times power. A shaped diode detector then interprets the 2 V maximum as four times power, and averages it out to the wrong power reading.

Another example shows how subtle signal imperfections can cause errors. Consider a CW signal with a harmonic signal –20 dBc (20 dB below the carrier amplitude or with a voltage equal to 10% of the carrier). Figure 4-12 shows a mathematical model of the increasing maximum error caused by a –20 dBc harmonic signal, as the carrier power level ranges from –30 to +20 dBm. While actual deviation from true power is a function of the phase difference between the carrier and its harmonic, the error limits are shown to be as high as 0.9 dB. If the harmonic was measured in the true square-law region, a –20 dBc harmonic represents only $1/100^{th}$ of the power of the carrier or 1% added power to the carrier.

It might also be observed that the design architecture of the PDB sensors utilizes a balanced, push-pull-diode configuration. This structure inherently rejects even-number harmonics of the RF input signal, therefore will provide 15 to 20 dB rejection of even-number harmonics above the square-law region.

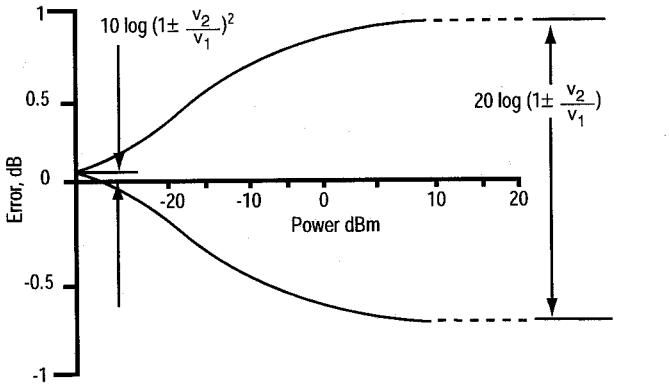

Figure 4-12. Estimated error limits for diode detectors operated above square-law range, for CW signal with –20 dBc harmonic.

Conclusion

Used with the EPM Series of power meters, the E9300 wide-dynamic-range average power sensors provide accurate power measurements for digitally modulated signals, multitone, and CW signals over a wider range of power levels (80 dB) than is currently achieved with traditional thermocouple or diode based power sensors. This is because their two path architecture keeps the detection diodes below their square-law limits.

The EPM Series of power meters, and E4412A and E4413A sensors, feature detector-shaping compensation to deliver dynamic range above square law (90 dB maximum), and should only be used for CW signals.

Average power measurements on pulsed and complex modulation signals can be measured using Agilent thermocouple sensors and EPM Series power meters. The 8480D-type diode sensors can be used below –20 dBm.

Peak and average sensor and meter technology described next in Chapter V provide accurate measurement of pulsed and complex modulation signals.

---

[1] S.M. Sze, *Physics of Semiconductor Devices*, Second Edition, Wiley, (1981).

[2] P.A. Szente, S. Adam, and R.B. Riley, "Low-Barrier Schottky-Diode Detectors," *Microwave Journal*, Vol. 19 No. 2 (Feb., 1976).

[3] R.J. Malik, T.R. Aucoin and R.L. Ross, "Planar-Doped Barriers in GaAs Molecular Beam Epitaxy," *Electronics Letters*, Vol 1G #22, (Oct., 1980).

[4] A. A. Fraser, "A Planar-Doped-Barrier Detector for General Purpose Applications," *Microwave Journal*, (May, 1987).

[5] US Patent #4943764, assigned to Hewlett-Packard Company

[6] Zurakowski, M, et al, "Diode Integrated Circuits for MM Applications," Hewlett-Packard Journal, Nov. 1986.

V. Peak and Average Diode Sensors and Instrumentation

Measuring and characterizing parameters of signals with pulsed and/or complex-modulation is simple in theory but difficult in practice. The simple part is that you detect the modulation envelope in a diode sensor and feed that wideband video to the power instrument for amplification. In the power meter instrument you again detect the modulation envelope with a 20-megasample/second (Msa/s) continuous sampling detector, making it a double-detection system.

The hard part actually gets taken care of by Agilent, by providing innovative hardware for the signal processing in the Agilent EPM-P power meters. The firmware and software accompanying those meters feature a whole series of complex corrections for various anomalies. For example, the first detection diode(s) have to handle signal levels from the square-law detection region, through the quasi-square law range into the linear ranges. These are compensated by a three-dimensional data matrix for frequency response and the transitional detection law versus power level. The data are measured and stored in each individual sensor EPROM. The data matrix also provides for temperature corrections since that parameter is pivotal in its sensor action.

Diode sensor technology is the ideal solution for characterizing high performance pulsed-modulation envelopes or complex digital formats. Since diode elements respond to fast video modulation, they easily provide detected video signals for amplification and measurement of the demodulated envelope parameters.

Agilent's peak and average power sensors and meters are specifically designed for video bandwidths as wide as 5 MHz. Besides pulsed and digital formats, this recommends them for additional applications such as two-tone tests (if tone separation is less than the sensor bandwidth) or full-channel signal formats that can exhibit statistical spikes in signals which average-sensing diode detectors may not integrate correctly. This chapter will describe the theory and practice of power measurements on these types of signals.

Traditional pulsed modulation formats

Most early pulsed system applications from the late 1930s were simple, rectangular formats for radiolocation (radar and navigation). In the military/aerospace technology race of the 1960s, pulsed formats became much more sophisticated. Radar and EW (countermeasures) transmitters moved from traditional pulsed formats to exploit complex and pseudo-random pulse-rate configurations for immunity to jamming and to reveal more precise data on unknown target returns. Simple computations with an average power measurement and duty cycle didn't work anymore.

Navigation systems such as air-traffic control (ATC) or distance measuring equipment (DME) have non-traditional pulse configurations too, such as pulse pairs, triplets or Gaussian-shaped envelopes to conserve frequency spectrum and avoid spectrum overlap in multiple aircraft environments. (A Gaussian-shaped envelope exhibits the interesting property that its spectrum has no side lobes, compared to the much-wider $\frac{\sin x}{x}$ side-lobe spectrum of a rectangular pulse.)

The now-discontinued Agilent 8990A peak power analyzer served for a time in the 1990s as the leading instrument for characterizing these and many other complex modulation formats. However, as the new wireless communication technologies of the mid-1990s accelerated rapidly, users needed power measurement equipment for wideband data transmission formats. This led to the present power measuring instruments and sensors which handle average power, as well as time-gated and peak power or peak-to-average ratios, with all those measurements delivered at very high measurement-data rates.

It's important to understand that the 5 MHz video bandwidth of Agilent's current peak and average sensors is not particularly well suited for modern radar or EW pulse formats, which feature rise and fall times in the nanosecond range. However, as will be shown in later pages, the time-gated function of the EPM-P meters is capable of averaging the power during the pulse-top period if the time-gate is set to bracket the radar pulse. It can also measure parameters such as the peak power, which in the case of a radar pulse, is usually the risetime overshoot. Other power spikes or parasitic oscillations would also qualify as a peak anomaly and be captured as peak power.

Complex modulation of wireless formats

Digital vector modulation became the modulation of choice as the digital revolution swept over RF and microwave communication systems some 20 years ago. The need to pack the maximum amount of digital data into the limited spectrum made it an obvious choice. For example, some early migrations of microwave terrestrial links from traditional analog frequency-division-multiplex (FDM), used 64 QAM (quadrature-amplitude-modulation) formats.

The advent of wireless communications technology in the 1990s accelerated the migration from analog to digital modulation formats. Then came an alphabet soup of digital modulation formats including, BPSK, QPSK, 8-PSK, 16 QAM, etc. Then came important variations such as π/4DQPSK and π/8-8PSK and others. But the breakthrough to successful cellular technology came with the sophisticated carrier switching of transmit signals. This permitted time-shared information to and from thousands of mobile subscribers, who were arrayed around in geographic regions (cells), communicating sequentially with one base station after another as the user's transceiver moved from cell to cell.

Some of those systems used data streams that featured time division multiple access (TDMA) technology, such as global system for mobile communication (GSM). Other system developers introduced a highly competitive code-division-multiple access (CDMA) format which includes IS-95 standards.

TDMA is the technology for time-sharing the same base station transmitter channel. Encoded voice data and new high data rate wireless links are modulated onto the transmitted carrier in the phase plane. These modulation formats create "constellations" of bit symbol locations such as shown in the π/8 shifted-8PSK configuration of Figure 5-1. This particular modulation format is used in the emerging Enhanced Data Rates for GSM Evolution (EDGE) systems which will offer high-speed data transfer over mobile wireless channels. By packing 3 bits per symbol, it increases data information rates, but thereby increases amplitude peak swings up to 16+ dB, making amplifier saturation more likely.

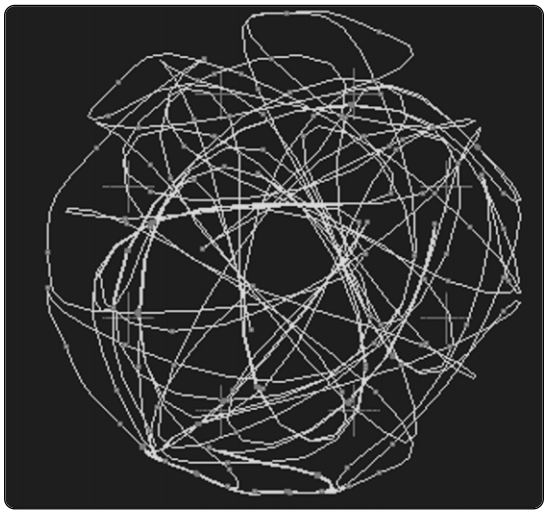

Figure 5-1. This π/8 8PSK digital modulation format is emerging for wideband data transmission on wireless channels, such as the EDGE technology.

In GSM, each TDMA wireless subscriber's share of time allows a useful data burst of say 524.6 µS, during which it is crucial for the power amplifier to remain below its saturation region. Driving the output stage into non-linear amplification causes the outermost phase states to compress, thereby increasing demodulation bit errors and lowering system reliability.

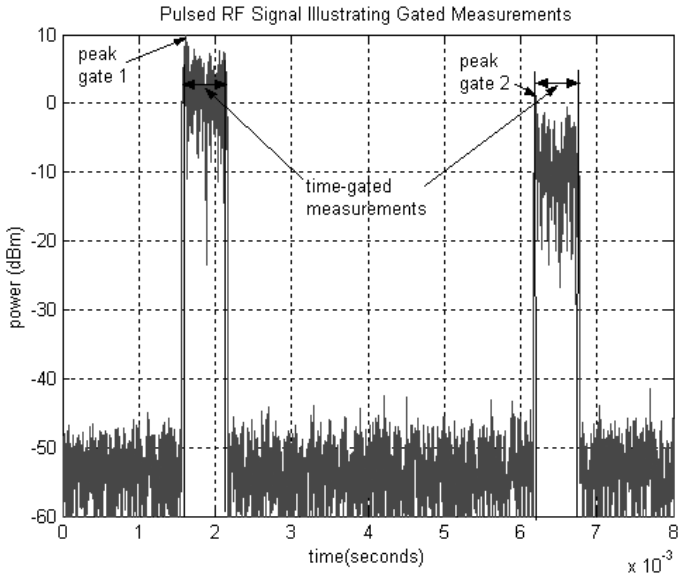

Figure 5-2. A time-domain oscilloscope shot of a wireless signal format, in this case, an EDGE signal in a GSM system. It is an ideal candidate for peak, average, and peak-to-average ratio measurements for time-gated wireless formats.

To make time-gated power measurements on TDMA type pulses, the measurement system must have sufficient rise and fall times. If overshoot is to be characterized, the power sensor rise/fall specifications must be fast enough to follow the rising and falling edges of the signal ON period. It is generally recommended that the power sensor should have a rise time of no more than 1/8 of the expected signal's rise time. Agilent's E9320 peak and average sensors have a 200 ns rise/fall time specification (E9323A and E9327A sensors with 5 MHz video bandwidth), which make them ideal for wireless TDMA formats.

The TDMA system feeds multiple carriers through a common output amplifier, which results in a transmitted power spectrum with almost white-noise-like characteristics. In contrast, CDMA encodes multiple data streams onto a single wider-band carrier using a pseudo-random code, with a similar transmitted power spectrum and similar power spikes.

Just like white noise, the average power of the transmitted signal is only one of the important parameters. Because of the statistical way that multiple carrier signal voltages can add randomly, instantaneous peak voltages can approach ratios of 10 to 30 times the carrier's rms voltage, depending on formats and filtering. This ratio, calculated with voltage parameters, is commonly called crest factor, and is functionally similar to the peak-to-average power ratio which is measured by Agilent peak and average power meters, described below.[1]

High peak-to-average power ratios imply dangers in saturation of the output power amplifiers. When saturation occurs, the outer bit-symbol locations compress, increasing bit errors and system unreliability. System designers handle this effect by "backing-off" the power amplifiers from their maximum peak ratings to assure that signal peak power operation is always within their linear range.

Wireless handsets also contain frequency-agile local oscillators that "hand-off" the mobile signal as it moves from ground cell to cell and links up to each new base-station frequency. Sometimes the transmitter power perturbations that occur during the frequency-switching transition also need to be characterized.

Other modern signal formats

Other application test signals cause problems for averaging diode sensors (above their square-law range) because of their complex spectrum content. For example, two-tone (or three-tone) test signals are often used for characterizing amplifiers for linearity of their amplification. If the amplification is non-linear, two pure input signals of $f_1$and f_2 result in intermodulation signals at the output, of the form $2f_1 - f_2$, $2f_2 - f_1$, and many more. The test is a very sensitive indicator of amplifier linearity.

Measuring power of such tones needs user analysis because the phase of the two carriers adds or cancels at the rate of the offset frequency. In a two-tone example, of V_1 and V_2, each with equal power, P, the constructive addition of tones results in a peak carrier of 2V, which is a peak power of 4P. An average-responding sensor would indicate 2P, but a peak-responding sensor would indicate 4P. It is the 2V effect that can saturate power amplifiers. When measuring peak power of such tone formats, the tone separation must be less than the sensor video bandwidth.

Other test signals, which contain high harmonic content, can also modify the carrier vector randomly and thus yield random power results. See the waveform analysis in Chapter IV.

Still other formats are generated by frequency-agile synthesizers, which can simulate entire, full-channel communications traffic formats. Since their component signals also add statistically, their power envelope is random. If the frequency spectrum of those power spikes fall within the sensor video bandwidth, they can be measured.

1. Accepted definition of crest factor (pulsed carrier): The ratio of the pulse peak (voltage) amplitude to the root-mean-square (voltage) amplitude.

Peak and average power sensing

The Agilent E9320 family of peak and average sensors demonstrates the current art of power sensing. See *Fundamentals Part 4* for product capability tables. They presently cover the 50 MHz to 6/18 GHz frequency ranges and –65 to +20 dBm power range. Ideal for comprehensive measurements on pulsed envelopes and signals with complex modulation, they also deliver data-corrected and reliable average power measurements. When teamed with the new Agilent EPM-P Series power meters (E4416A/17A), the combination can handle test signal envelopes with up to 5 MHz video bandwidth.

The basic block diagram for Agilent peak and average sensor is shown in Figure 5-3. It features parallel amplification paths, one for CW (average-only) and one for video (normal). Both modes use the same micro-circuit diode-sensor (bulkhead) element at the RF input. Signal processing in the two amplification paths is optimized to their differing needs for selecting the video bandwidths, filtering, chopping and other data requirements. Amplification is distributed, with an optimum gain in the sensor unit and more in the meter.

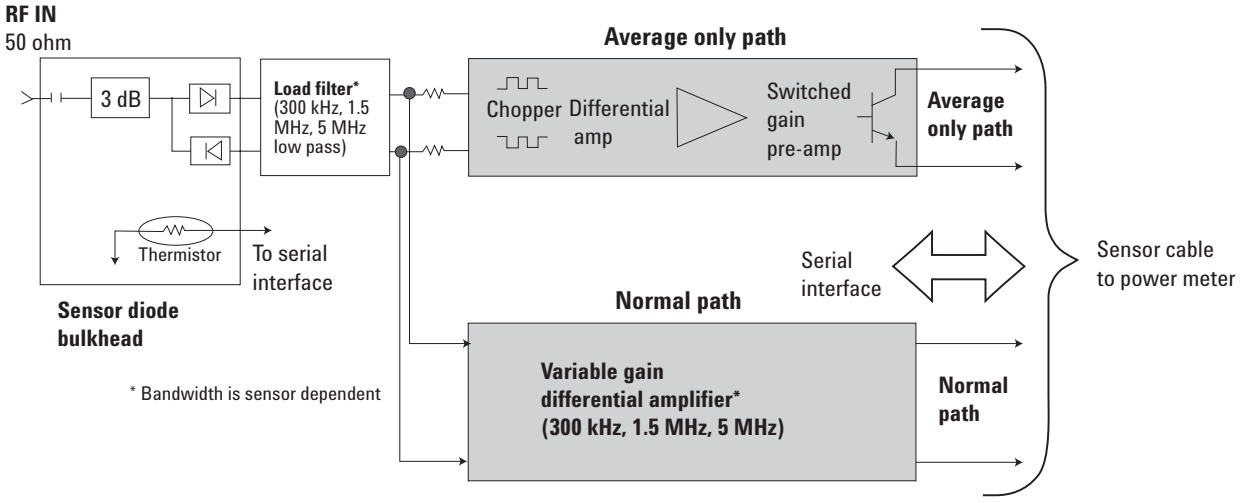

Figure 5-3. Simplified block diagram of the E9320 Series peak and average sensor, showing the parallel amplification paths, along with control lines and a temperature-sensing thermistor function, which corrects the diode's data.

In the average-only mode, amplification and chopping parameters are much the same as in previous Agilent averaging sensors, with typical dynamic power range of –65 to +20 dBm. In the normal (pulsed) mode, a separate-path dc coupled amplifier provides three sensor dependent maximum bandwidths of 300 kHz, 1.5 MHz, or 5 MHz, allowing the user to match the test signal's modulation bandwidth to the sophisticated instrument data processing. These considerations will be discussed later in this chapter.

Several functions are included in these peak and average sensors that are not available in most other diode sensors. First, all E-Series sensors have temperature corrections to improve stability and accuracy, with the correction data stored in an on-board EEPROM. The temperature-sensing thermistor element is mounted inside the bulkhead unit on the same microcircuit as the RF diode sensing elements.

Secondly, the peak and average sensors communicate with the E4416/7A meters using the serial bus shown. It is bi-directional to allow calibration data to upload to the meter whenever a new sensor is connected. Sensor cal data can even flow through the meter out the GPIB port for external computer purposes. In the other direction, the serial bus delivers control commands to the sensor, for example, to select which amplification path is to be activated.

Diode sensors used for peak pulse detection necessarily operate up into their linear detection regions and have various deviations from ideal. Power linearity is frequency dependent in the E9320 family, and the diodes also have some temperature dependence. Figure 5-4 shows how the EEPROM, resident in each sensor, stores the three-dimensional correction data that is derived from a special sensor calibration system at Agilent's factory and service facilities. The calibration process includes a data run in a temperature oven, during which time the input power is ramped over the critical power and frequency range at each calibration temperature.

Consider one axis of the temperature response in Figure 5-4 to be the frequency response, and the other axis to be the response to the power dynamic range. The "warped" surface profile therefore represents a single temperature, so many such surfaces of data exist in the EEPROM.

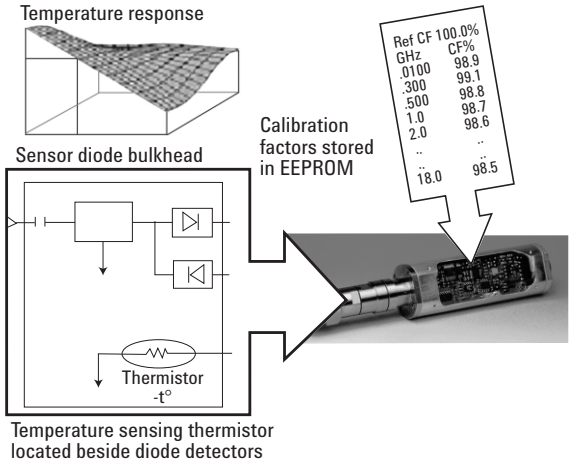

Figure 5-4. Temperature, power and frequency correction data, stored in each E9320-family peak and average sensor, uploads into the meter each time a new sensor is connected to the meter, dramatically improving measurement accuracy and confidence.

EPM-P Series power meters

Figure 5-5 shows an overview block diagram for the E4416A (single channel) power meter. Under microprocessor control, all the various functional components from panel keyboard to the logic and digital signal processor (DSP) functions are coordinated. For the average-only mode, signal processing is similar to previous meters. In fact, the EPM-P Series meters will accommodate all older Agilent thermocouple and diode sensors (but naturally won't read peak power). A 16-bit analog-to-digital converter (ADC) processes the average power signal.

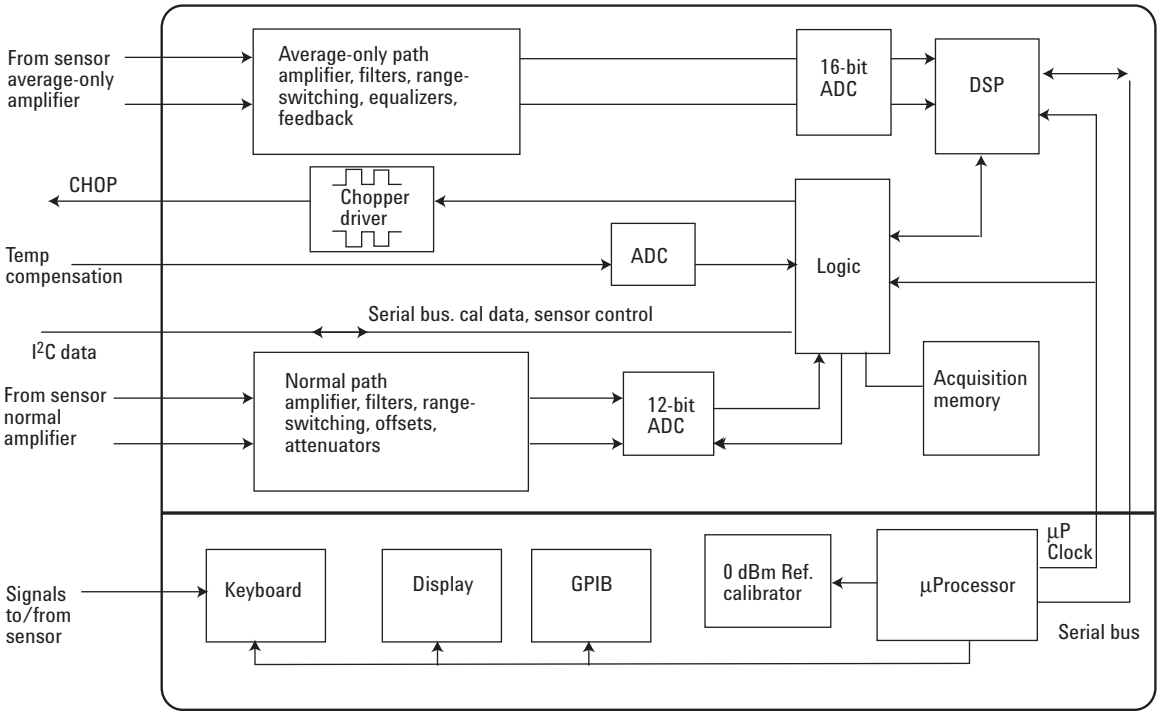

Figure 5-5. Simplified block diagram for E4416A shows extensive use of digital signal processing and control. Measurement confidence results from the comprehensive data correction routines.

A highly-sophisticated video amplifier design is implemented for the normal path to preserve modulation envelope fidelity and accuracy. Innovative filtering and range-switching, as well as differential offset controls and zeroing functions are handled. A 12-bit ADC processes the amplified envelope into a data stream for the DSP.

The “second detection” process, which is the crucial envelope detection phase, is implemented in the EPM-P meters with a sophisticated 20 Msa/s ADC running with 12-bit precision, as shown in the diagram of Figure 5-5.

There is a tradeoff in sampling strategy between continuous and random sampling processes. The EPM-P power meters feature continuous sampling at 20 Msa/s to ensure that all the peaks are captured, even on a single shot signal, therefore giving a true peak power reading. In simple terms, continuous sampling is quicker at building up the trace display compared to random sampling because you don’t have to build-up the trace over several iterations of the periodic signal, thus the single-shot capability.

Continuous sampling also allows for a digital filtering architecture and bandwidth correction within the power meter. Digital filtering in the EPM-P, the high, medium and low bandwidth settings, enhances the dynamic range of the meter/sensor combination. Its bandwidth correction provides optimum accuracy for peak and statistical power measurements.

Other meters that employ random sampling have somewhat more ability on larger bandwidth signals. For example, a random sampling rate of 2.5 to 5 Msa/s might yield a 10 MHz bandwidth; contrasted to the Agilent EPM-P power meter continuous method of 20 Msa/s delivers a 5 MHz video bandwidth. Random sampling is also claimed to minimize aliasing effects, but Agilent concluded that was an infrequent issue.

On balance, Agilent chose continuous sampling because it won’t miss data, can characterize single shot power pulses, and provides substantially higher measurement data rates for important production test applications. To illustrate the measurement data transfer rates, which are achievable with the continuous sampling design, Table 5-1 shows the readings/second when using the GPIB.

Table 5-1. Impressive GPIB measurement data rates are available with the EPM-P meter.

Sensor type		**Measurement speed** (readings/second)		
		Normal	**x 2**	**Fast**
E-Series E9320 peak and average sensors	Average Only mode	20	40	400
	Normal mode	20	40	1000
E-Series CW and E9300 average power sensors		20	40	400
8480 Series sensors		20	40	N.A.

EPM-P Series power meters are compatible with all 8480 and E-Series power sensors. If you need average power only and fast measurement speed, the EPM-P power meters provide a speed advantage compared to the EPM meters (E4418B and E4419B). The E-Series CW (E4412A/13A) and E9300 average power sensors have a maximum speed, in FAST mode, of 400 readings per second with the EPM-P meters. That’s a doubling in measurement speed compared to the EPM meters.

To achieve 1,000 readings/second, over the GPIB, the EPM-P power meter must be used with an E9320 power sensor. The E9320 power sensor is configured to operate in Normal mode in free run acquisition and the EPM-P power meter should be configured to operate in FAST mode. When operating in FAST mode, the limiting factors tends to be the speed of the controller being used to retrieve the results from the power meter, and to a certain extent, the volume of GPIB traffic. Returning the results in binary format (SCPI command FORMat REAL) will reduce the volume of GPIB traffic. The speed of the associated controller is a combination of the hardware platform and the programming environment being used.

Note: When operating in FAST mode, averaging, limits and ratio/difference math functions are all disabled.

To ensure the maximum speed performance when using the EPM-P power meter, the following factors should be considered:

Units: The power meter can output results in either linear (W) or log units (dB). The internal units are linear and therefore optimal performance will be achieved when the results output are also in linear units (since the overhead of performing a log function is removed).

Command: The FETCh command must be used to return a result, as low-level commands will ensure the best speed performance.

Trigger Mode: Free Run, as it continuously takes measurements on this channel.

Trigger Count: To get the fastest measurement speed the trigger count must be set to return multiple measurements for each FETCh command. To attain 1000 readings/second a count of 50 is required (max GPIB width).

Output Format: The Real format is required for FAST mode as a means to reduced bus traffic, by returning the output in binary format.

The central function for peak and average power meters is to provide reliable, accurate, and fast characterization of pulsed and complex modulation envelopes. The EPM-P meters excel in versatility featuring a technique called time-gated measurements. For a descriptive example, Figure 5-6 shows four typical time-gated power measurements on a GSM signal.

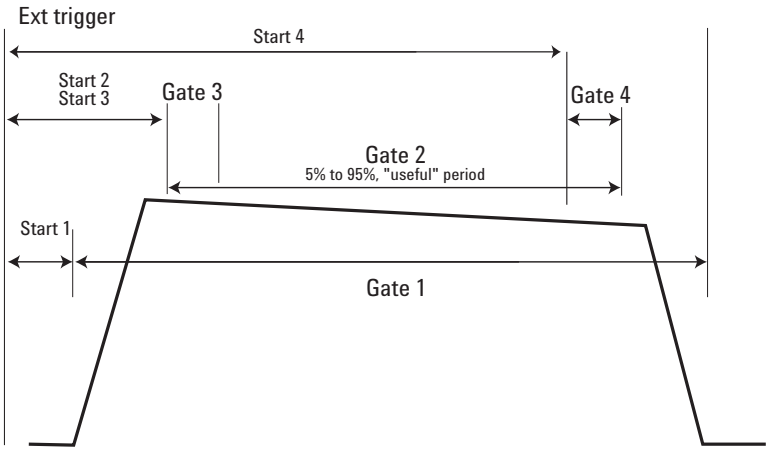

Figure 5-6. For this typical GSM pulse, time-gated measurement techniques permit the EPM-P meter user to configure four different measurement gate periods, each with its own delay time, measured from a "trigger-point" pulse.

In Figure 5-6, Gate 2 provides the burst average power over the "useful" GSM time period, which is in essence the averaged power during the gate period, at the top of the pulse. It is therefore very similar to the *Fundamentals Part 1* definition of pulse-top amplitude, although pulse-top is defined between the half-power points. Remember that each gate may be programmed to measure peak or average or ratio.

In this example, Gate 1 captures the peak power during its complete Gate 1 period. In the E4416A, this definition of peak power is equivalent to the *Fundamentals Part 1* definition of peak power, which is the highest instantaneous power spike to occur during the open measurement gate period. Functionally, the peak power data allows the user to measure the saturation effect that power spike overloads create in test amplifier performance.

The E4416/7A meters measure three different selectable parameters during each gate, peak power, average power and peak-to-average ratio. Thus, an industry-important peak-to-average ratio may be made during the same gate time, or conversely, the ratio of peak power in one gate time may be computed against the average power in another gate time.

A pulse droop measurement can be obtained by subtracting the two powers, Gate 3 – Gate 4. All three of these measurements can be simultaneously displayed on the four-line numeric liquid-crystal display (LCD) screen, along with the peak power from Gate 1.

The trigger point may be selected from three sources, 1) an external pulse, 2) derived internally, digitally, from the measured pulse envelope, or 3) from the external GPIB source. The acquisition modes may be single, continuous or free-run. Other trigger manipulations are also featured, such as holdoff or delay. Once the trigger point is set, it may be output to other system instrumentation via a rear BNC connector.

Current models of the EPM-P power meters feature pre-defined software/ firmware measurement routines for eight popular wireless signal formats, including GSM-900, EDGE, iDEN, NADC, cdmaOne, cdma2000, W-CDMA, and Bluetooth™. The following example is that for the GSM pre-defined measurement setup.

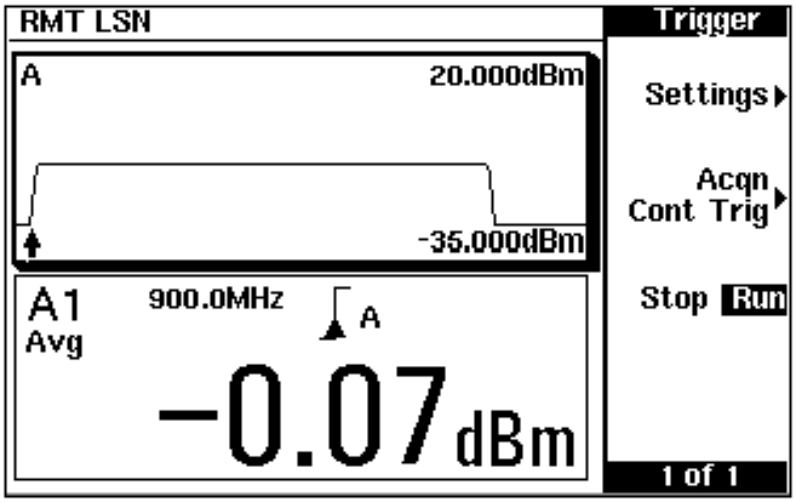

Figure 5-7. The pre-defined GSM routine takes 10,400 data samples in the time-gated period.

The pre-defined setups are one-button controls, which makes the instrument setup more convenient and enables users to actually making measurements quicker. For example, the pre-defined GSM setup has a gate length of 520 µsec. With a sampling rate of 20 Msa/s, that's 10,400 samples within the time-gated period. To find out the number of samples taken in any gate length, simply divide the length (in seconds) by 50^{-9}.

On the screen, 234 pixels are used to generate the trace display, as shown in Figure 5-7. The height per window (two windows maximum for the whole display) in pixels is 85 of which 57 are used for the trace display.

Computation power–gated data concept

The signal processing in the E4416/7A meters has been designed to provide exceptional data computation and display versatility. Figure 5-8 shows the data paths for the four independent gate periods, each with its own delay time. Each gate can be set to measure average, peak, and peak-to-average power data.

Each gate can then manipulate those three parameters into two computed parameters (F-feeds) such as F1 minus F2 or F1/F2, to be displayed in one of the four window partitions. The block shown as the “measurement highway” takes care of moving data to the user-configured display line on the LCD. The highway also permits computation of shared data between the four gates.

This computational power is particularly valuable in TDMA wireless test scenarios such as GSM, GPRS, EDGE, and NADC, where various simultaneous combinations of computed parameters are required.

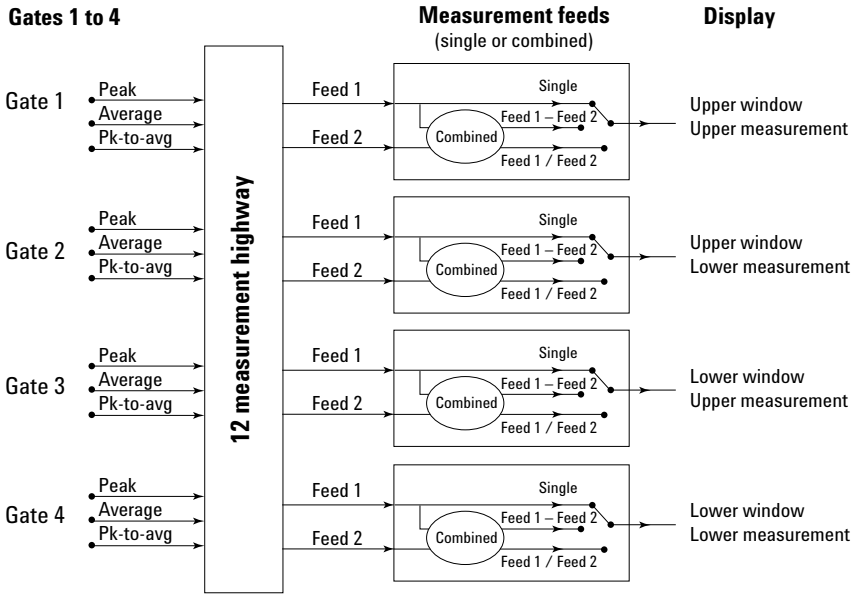

Figure 5-8. User-configured data manipulations are a major feature of the EPM-P series power meters.

The large LCD display partitions up to four-line formats to help interpret and compare measurement results, using the measurement highway. The user can also select large character readouts to permit viewing from a distance. For example, Figure 5-9(b) shows how the four lines could be configured to display average power in dBm and W, peak power and peak-to-average ratio.
The user can also choose to show the analog power envelopes for two selected traces in the partitioned display. Figure 5-9(a) shows the user set-up display for four gate periods and delays.

It should be noted that all the above configurations for feeding actual data plus computed data, such as power ratios, through the measurement highway is for a single sensor. When using the E4417A dual-power meter, the second sensor provides a doubling of retrieved power data, all of which may be user-selected to create combined ratios or power differences between sensor A and sensor B channels.

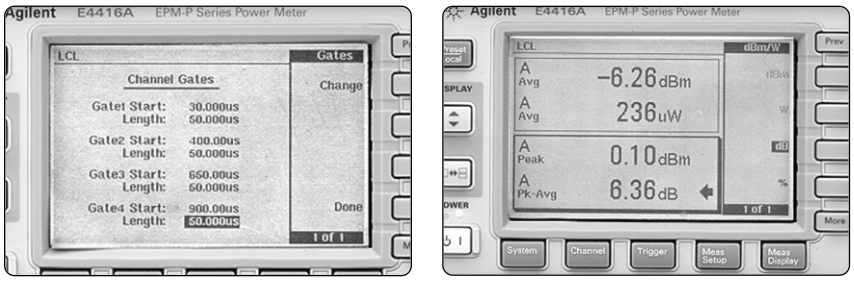

(a) (b)

Figure 5-9. The back-lighted LCD display delivers powerful readout versatility: (a) shows how the user sets the delay and measurement times for each of four gates, (b) shows a simultaneous display of four Gate A parameters; average power in dBm and µW, peak power, and peak to average ratio. The user could also choose a digitally-derived pulse envelope representation as well.

This may be a good juncture to consider power data averaging. The EPM-P does not have averaging for making peak power measurements. Peak power is by definition a single occurance defined as the maximum instantaneous power of the signal-under-test, therefore averaging is not appropriate.

In terms of average power measurements, there are different ways to do the averaging. In Normal operation the instrument shows a computed moving average. For example, for an average of eight, when a new value is measured it is averaged with the previous seven readings. If you want a “block” average, where you take eight measurements and average them, then take another eight measurements and average them, you can use the TRIG:DEL:AUTO ON command. In that command the meter inserts a settling time before taking the measurement. The average is adjustable and can be set by the user or it can be auto averaged, which depends on the sensor and the power level, being measured. Auto averaging will increase the averaging as you get lower down in power, to minimize display jumping.

When measuring a pulsed signal, video averaging can be used. For example, averaging on a GSM signal, the number of averages is actually the number of pulses of the given setup - if you are making a measurement in timeslot 1 with eight averages it will average the next eight measurements of timeslot 1.

Video bandwidth considerations

Pity the Agilent amplifier designer of the EPM-P peak power amplifier chain. Inside the diode sensor, values of R and C in the Figure 4-3 equivalent circuit have conflicting demands placed on them. For maximum detection sensitivity and dynamic range, R should be large. And for maximum RF input frequency range, C should also be large. However, for maximum detection flatness and stability of the video bandwidth, R and C should both be small. In addition, there are optimum values of R and C for linearity, temperature stability and mismatch. Other tradeoffs arise when considering low-input frequency (down to RF) range limits versus wide video bandwidth.

So optimizing for one set of sensor criteria would have the effect of severely impacting other key sensor specifications for users. Agilent has taken the approach to introduce a family of E9320 sensors specifically optimized for maximum dynamic range and also to minimize errors for specific wireless standards, as follows:

- E9321A/25A: 300 kHz video bandwidth for GSM and EDGE
- E9322A/26A: 1.5 MHz video bandwidth for CDMA (IS-95), and
- E9323A/27A: 5 MHz video bandwidth for W-CMDA applications.

One instance where the conflicting demands on load circuit components becomes apparent is when we consider the trade-off between the low frequency RF range and wide video bandwidth. To remain sensitive at low input frequencies (< 100 MHz), high load resistance and capacitance are optimal. However, wide video bandwidth requires low values for these components. This leads to a compromise between variations in video bandwidth and the frequency dependence of sensor linearity.

Table 5-2 displays the complete user parameter tradeoffs for the available peak and average sensors, including video bandwidth and peak power dynamic range. In cases when users need to measure the power of multiple signal types with a single sensor model, they can consider the dynamic range of the bandwidth settings. With this information, they can determine if they require only one sensor or need to obtain multiple sensors for their application.

The filter video bandwidths stated in the table are not the traditional 3 dB bandwidths, since these video bandwidths are optimized and corrected for optimal flatness. Detailed response curves are shown in the product specifications (see product reference literature on the Agilent Website). Video filter characteristics are measured using a technique of applying a two-tone signal, programming the power meter for a peak to average measurement, then increasing the separation of the two-tones until a frequency response curve is generated. With such a procedure, the curve shape is not a traditional roll-off characteristic.

Table 5-2. E9320 sensor bandwidth versus peak power dynamic range (normal mode).

Sensor model	**Modulation bandwidth / Max. peak power dynamic range**			
6 GHz/18 GHz	**High**	**Medium**	**Low**	**Off**
E9321A/E9325A	300 kHz/–42 to +20 dBm	100 kHz/–43 to +20 dBm	30 kHz/–45 to +20 dBm	–40 dBm to +20 dBm
E9322A/E9326A	1.5 MHz/–37 to +20 dBm	300 kHz/–38 to +20 dBm	100 kHz/–39 to +20 dBm	–36 dBm to +20 dBm
E9323A/E9327A	5 MHz/–32 to +20 dBm	1.5 MHz/–34 to +20 dBm	300 kHz/–36 to +20 dBm	–32 dBm to +20 dBm

If the video bandwidth is not sufficiently flat, errors will be introduced in peak power measurements. The wider the video bandwidth, the greater the variation in linearity. In traditional wide-dynamic range sensors with minimal video bandwidth, only a 50-MHz linearity calibration is required. Figure 5-10 shows how only one frequency linearity correction at 50 MHz (50 MHz is the flat line at 0 dB) will lead to linearity errors for sensors with a wide video bandwidth.

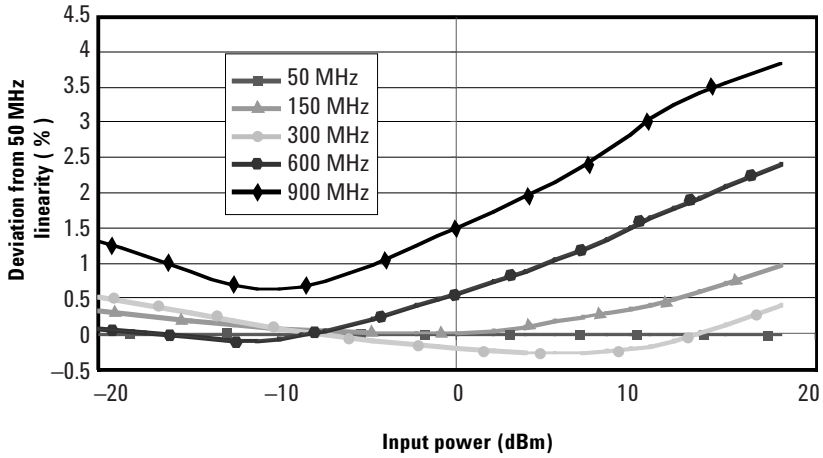

Figure 5-10. The frequency-dependent linearity of a wide video-bandwidth sensor is shown for various input frequencies from 50 to 900 MHz.

To achieve a wide, flat video bandwidth without compromising linearity, a frequency-dependent linearity correction (FDLC) has been implemented in the E9320 sensors. These sensors are factory calibrated at 50 MHz and at key frequency points up to 900 MHz in order to provide the correction data for the FDLC. This addresses the trade-off in linearity and video bandwidth, but it still leaves the bandwidth susceptible to power and temperature variations in the detection diode's resistance. The dc-coupled amplifier in the sensor's Normal mode path has a different gain for each video bandwidth, the highest gain is employed in the 300 kHz sensors.

The result of all this care is that conflicting tradeoffs have been corrected in all possible cases by use of the internal stored data matrix.

All the above shows that when instrumenting for peak power measurements, it is crucial to analyze the effect of the instrumentation video bandwidths on the accuracy of the resulting data. Agilent E4416/17A meters have been optimized to avoid degrading key specifications like linearity, mismatch, dynamic range and temperature stability. For further information on this matter, see the following article; "Power Measurements for the Communications Market."[1]

Versatile user interface

The E4416A/17A meters feature a user-friendly interface and powerful display controls. Hardkeys control the most-frequently used functions such as sensor calibration and triggering, while softkey menus simplify configuring the meter for detailed measurement sequences. A save/recall menu stores up to ten instrument configurations for easy switching of test processes.

Measurement considerations for traditional peak pulses

Modern radars and navigation systems have moved to narrower pulses, which permitted better separation of multiple targets or improved target resolution. Then came even newer technologies for pulsing with longer—but phase coded—formats that allowed for determining things like shape or size of targets. Multiple pulses and random pulse repetition rates are design strategies for resistance to countermeasures jamming.

All of these different directions of pulse power technologies means that specifying a measurement power meter requires a clear knowledge of the key parameters that need to be characterized. For some test sequences, measurement of the numerous pulse power and time parameters performed by full peak power analyzers may be needed. On others, only pulse-top and average power measurements are required, for which Agilent average or peak and average sensors will suffice.

Design and production test for pulsed systems often require measurements of both peak pulse power (pulse top) as well as average power for the transmitter and other internal system components. Thermal sensors inherently respond to total average power, as long as the peak power excursions do not exceed the peak ratings of the sensor. By knowing the precise measurement specification, a test engineer might use a simpler and less expensive power meter to determine that a subsystem is operating to its proper performance envelope.

The Agilent E9320 sensor family (using the EPM-P meter) can provide highly accurate and useful data for parameters such as pulse top or average power on pulses as narrow as 300 ns. While not specifically intended for narrow pulse characterization, its 5 MHz bandwidth amplifiers can deliver the measurements of Table 5-3. [2]

Table 5-3. E9323A/27A power sensors can measure pulse parameters.

Key pulse parameter	EPM-P/E9320 specifications
Rise time	200 ns
Fall time	200 ns
Minimum pulse width	300 ns
Pulse repetition rate	2 MHz
Pulse repetition interval	500 ns

Analysis software package for complex modulation manipulations
An important development for product development and verification engineers is a powerful VEE analyzer software package that places the EPM-P meter totally in control of the PC or laptop. This EPM-P VEE software package is available free of charge.[3] It operates via the GPIB, and provides the statistical, power, frequency, and time measurements that are required for CDMA and TDMA signal formats. The CD-ROM package includes a VEE installation program.

The statistical package includes the ability to capture

- cumulative distribution function (CDF)
- complementary CDF (CCDF or 1-CDF)
- probability density function (PDF)

These are crucial diagnostic parameters for system signals like CDMA formats. Figure 5-11 shows a typical distribution function display. Analyzing such power distribution computations can reveal how a power amplifier may be distorting a broadband signal that it is transmitting. Or a baseband DSP signal designer can completely specify the power distribution characteristics to the associated RF subsystem designers. For example, for Figure 5-11, the data shows that for 0.3% of the time, the signal power is at or above 8 dB peak-to-average ratio.

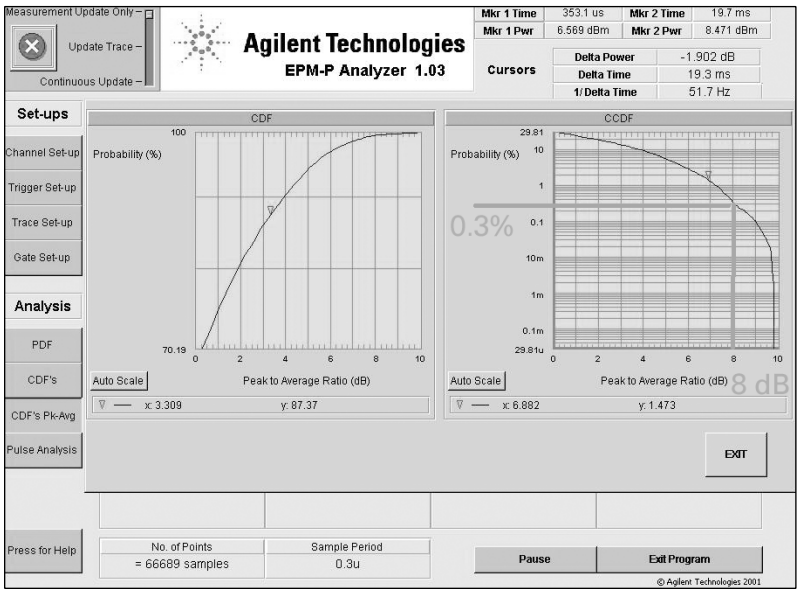

Figure 5-11. On this CCDF analysis screen, the Y-axis shows the percentage of time the wireless signal power is at or above the power specified by the X-axis.

For traditional pulse work, the analysis package also includes a powerful pulse characterization routine. It computes and displays the following power parameters: pulse top, pulse base, distal, mesial, proximal, peak, average, peak/average ratio, burst average, and duty cycle. It does the same for these time and frequency parameters: rise time, fall time, pulse repetition frequency (PRF), pulse repetition interval (PRI), pulse width and off time. All of these pulsed power parameters were originally defined with the 1990 introduction of the Agilent 8990A peak power analyzer, and are described in Chapter II of *Fundamentals Part 1.*

Special peak sensor calibration for temperature and range

As mentioned in several previous chapters, Agilent E9320-Series peak and average sensors require a three-dimensional matrix of correction data to deliver their highest possible measurement accuracy. The production test systems run the input power throughout the frequency range and the power range of the specified limits of the sensor. Since the sensor detection characteristics are sensitive to operating temperature, the sensor is also subjected to a temperature run which stores those correction data as well.

When factory tested, the internal ROM stores the correction data, which is useful for a long period of time, since the internal components do not exhibit much aging. For user metrology labs which are required to re-verify sensors periodically, it is recommended that they treat the various families of sensors differently.

Thermistor and thermocouple—heat sensing technology—and older diode sensors such as the 8481D family can have their calibration factors verified using the standards procedures, usually the power splitter method covered in early chapters. Changes to the calibration factors can be altered on the sensor's printed cal factor label and calibration certificate.

E-Series sensors, such as the E4412A/13A and the E930x-Series can have their cal factors verified, and can have their correction data "re-burned," although these tests are usually run only at room temperature, since the temperature corrections are assumed not to change with time. These verification runs should be made with the corrections function turned on. Naturally if a sensor has been subject to observable abuse, deeper testing might be needed.

E9320 peak and average sensors can be verified but should not attempt re-burn of correction data. The correction algorithm of the peak and average sensors is logically more complicated, and cal factor runs without temperature characterization will compromise the measurement uncertainty.

For external calibration laboratories with significant test loads of power sensors, it is recommended that you contact Agilent's support organization, which can furnish you with considerable detail on test recommendations for each sensor family type.

Recent research on linearity and pulse-shape characterization of peak and average sensors

For some decades now, the power measurement industry has offered peak power analyzer instrumentation without direct traceability of the peak power parameters to NMIs. This was a result of low priorities of NMI research funding related to measurement uncertainty needs in the peak sensing products. Industry improvised with measurement configurations that carefully compared peak power sensors under calibration with average sensor/meter combinations with known standardized and traceable power certifications.

However, with the rapid rise of complex and pulsed formats in the wireless communications industry, the need for highest-level standards for peak power became evident. Accordingly, for the past several years, the NPL in the UK has undertaken projects to provide characterization of peak and average sensors, plus a provision of measurement services for traceability of peak parameters of power sensors.

As of this writing, the National Physical Laboratory (NPL) in the UK has sponsored a research program into the complexities of characterizing peak power sensors. These are not trivial considerations because bandwidth of the instrumentation and the linearity of the sensor both contribute to computed errors. In particular, sensor linearity at low power levels was generally poorer than CW sensors. This can lead to uncertainties in computed data such as peak-to-average power and power statistics that are required for CDMA systems like cdmaOne and W-CDMA. [4]

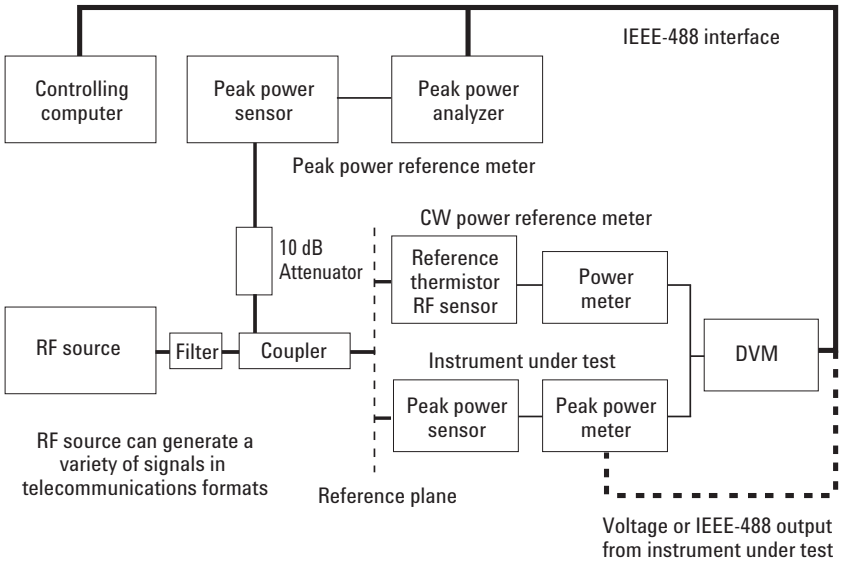

Graphic courtesy of NPL, Teddington, UK (3rd RF Wireless Measurements Forum: 25 July 2000)

Figure 5-12. NPL (UK) peak power measurement system.

The NPL calibration system of Figure 5-12 was validated against sampling oscilloscope measurements, which provided an alternate method to characterize the waveform characteristics of the pulsed RF signal. This is important because of the generally limited bandwidth of the peak power instrumentation associated with pulsed or complex-modulation power signals. Of course, the ultimate power standard was still a CW sensor, which served as the traceable link to the NPL power standard.

For users who require additional information on peak power traceability, visit the NPL website. [5]

[1] Anderson, Alan, "Power Measurements for the Communications Market," *MW/RF Magazine*, October, 2000.

[2] AN1438, "EPM-P Series Power Meters Used in Radar and Pulse Applications," Agilent Technologies, literature number 5988-8522EN.

[3] CD-ROM: EPM and EPM-P Series Power Meters, part number E4416-90032.
This CD-ROM contains the power meters and sensors Learnware (User's Guides, Programming Guides, Operating Guides and Service Manuals). The CD-ROM also contains technical specifications, data sheets, product overviews, configuration guide, application and product notes, power meter tutorials, analyzer software for the EPM-P power meters, IVI-COM drivers, IntuiLink toolbar for the EPM power meters and VXI Plug & Play drivers for the EPM power meters.

This versatile CD-ROM package is shipped free with every EPM and EPM-P Series power meter. Most of the information is also available at: www.agilent.com/find/powermeters.

[4] Holland, K., and Howes, J., "Improvements to the Microwave Mixer and Power Sensor Linearity Measurement Capability at the National Physical Laboratory," (In the UK) IEE Proc.-Sci Meas. Technology, Nov. 2002.

[5] Website for National Physics Laboratory, Teddington, UK, pulsed power information (note caps): www.npl.co.uk/measurement_services/ms_EG.html#EG04

Agilent Technologies' Test and Measurement Support, Services, and Assistance
Agilent Technologies aims to maximize the value you receive, while minimizing your risk and problems. We strive to ensure that you get the test and measurement capabilities you paid for and obtain the support you need. Our extensive support resources and services can help you choose the right Agilent products for your applications and apply them successfully. Every instrument and system we sell has a global warranty. Support is available for at least five years beyond the production life of the product. Two concepts underlie Agilent's overall support policy: "Our Promise" and "Your Advantage."

Our Promise
Our Promise means your Agilent test and measurement equipment will meet its advertised performance and functionality. When you are choosing new equipment, we will help you with product information, including realistic performance specifications and practical recommendations from experienced test engineers. When you use Agilent equipment, we can verify that it works properly, help with product operation, and provide basic measurement assistance for the use of specified capabilities, at no extra cost upon request. Many self-help tools are available.

Your Advantage
Your Advantage means that Agilent offers a wide range of additional expert test and measurement services, which you can purchase according to your unique technical and business needs. Solve problems efficiently and gain a competitive edge by contracting with us for calibration, extra-cost upgrades, out-of-warranty repairs, and onsite education and training, as well as design, system integration, project management, and other professional engineering services. Experienced Agilent engineers and technicians worldwide can help you maximize your productivity, optimize the return on investment of your Agilent instruments and systems, and obtain dependable measurement accuracy for the life of those products.

Agilent Email Updates

www.agilent.com/find/emailupdates
Get the latest information on the products and applications you select.

Agilent T&M Software and Connectivity
Agilent's Test and Measurement software and connectivity products, solutions and developer network allows you to take time out of connecting your instruments to your computer with tools based on PC standards, so you can focus on your tasks, not on your connections. Visit **www.agilent.com/find/connectivity** for more information.

By internet, phone, or fax, get assistance with all your test & measurement needs

Phone or Fax
United States:
(tel) 800 452 4844
Canada:
(tel) 877 894 4414
(fax) 905 282 6495
China:
(tel) 800 810 0189
(fax) 800 820 2816
Europe:
(tel) (31 20) 547 2323
(fax) (31 20) 547 2390
Japan:
(tel) (81) 426 56 7832
(fax) (81) 426 56 7840

Korea:
(tel) (82 2) 2004 5004
(fax) (82 2) 2004 5115
Latin America:
(tel) (305) 269 7500
(fax) (305) 269 7599
Taiwan:
(tel) 0800 047 866
(fax) 0800 286 331
Other Asia Pacific Countries:
(tel) (65) 6375 8100
(fax) (65) 6836 0252
Email: tm_asia@agilent.com

Online Assistance:
www.agilent.com/find/assist

Product specifications and descriptions in this document subject to change without notice.

Printed in USA *April 21, 2003*
5988-9214EN

Agilent Technologies